U.S. DEPARTMENT OF COMMERCE
National Technical Information Service

PB-274 011

High Sensitivity Fourier Transform NMR Intermolecular Interacting Between Environment Toxic Substances and Biological Macromolecules

Florida State Univ., Tallahassee

Prepared for

Health Effects Research Lab., Research Triangle Park, N.C.

Sep 77

PB 274 011

EPA-600/1-77-045
September 1977

Environmental Health Effects Research Series

UNITED STATES ENVIRONMENTAL PROTECTION AGENCY

REPRODUCED BY
NATIONAL TECHNICAL
INFORMATION SERVICE
U. S. DEPARTMENT OF COMMERCE
SPRINGFIELD, VA. 22161

RESEARCH REPORTING SERIES

Research reports of the Office of Research and Development, U.S. Environmental Protection Agency, have been grouped into nine series. These nine broad categories were established to facilitate further development and application of environmental technology. Elimination of traditional grouping was consciously planned to foster technology transfer and a maximum interface in related fields. The nine series are:

1. Environmental Health Effects Research
2. Environmental Protection Technology
3. Ecological Research
4. Environmental Monitoring
5. Socioeconomic Environmental Studies
6. Scientific and Technical Assessment Reports (STAR)
7. Interagency Energy-Environment Research and Development
8. "Special" Reports
9. Miscellaneous Reports

This report has been assigned to the ENVIRONMENTAL HEALTH EFFECTS RESEARCH series. This series describes projects and studies relating to the tolerances of man for unhealthful substances or conditions. This work is generally assessed from a medical viewpoint, including physiological or psychological studies. In addition to toxicology and other medical specialities, study areas include biomedical instrumentation and health research techniques utilizing animals — but always with intended application to human health measures.

This document is available to the public through the National Technical Information Service, Springfield, Virginia 22161.

TECHNICAL REPORT DATA

(Please read Instructions on the reverse before completing)

1. REPORT NO. EPA-600/1-77-045	2.	3. RECIPIENT'S ACCESSION NO. PB274011
4. TITLE AND SUBTITLE HIGH SENSITIVITY FOURIER TRANSFORM NMR. Intermolecular Interactions Between Environmental Toxic Substances and Biological Macromolecules		5. REPORT DATE September 1977 6. PERFORMING ORGANIZATION CODE
7. AUTHOR(S) George C. Levy		8. PERFORMING ORGANIZATION REPORT NO.
9. PERFORMING ORGANIZATION NAME AND ADDRESS Department of Chemistry The Florida State University Tallahassee, FL 32306		10. PROGRAM ELEMENT NO. 1EA615 11. CONTRACT/GRANT NO. 803095
12. SPONSORING AGENCY NAME AND ADDRESS Health Effects Research Laboratory RTP, NC Office of Research and Development U.S. Environmental Protection Agency Research Triangle Park, N.C. 27711		13. TYPE OF REPORT AND PERIOD COVERED 14. SPONSORING AGENCY CODE EPA 600/11
15. SUPPLEMENTARY NOTES		

16. ABSTRACT

This project explored the feasibility of developing new techniques for evaluation of the effects of environmental toxic materials on complex biopolymer systems using high sensitivity Fourier transform nuclear magnetic resonance (nmr) spectroscopy. Commercial instrumentation available in 1974-75 did not possess adequate sensitivity, and thus one goal of this project was to increase spectral sensitivity, especially for the ^{13}C and other nuclides having low magnetogyric ratios. Initially, modifications to an existing Bruker HX-270 spectrometer provided moderate improvement in sensitivity for ^{13}C and substantial sensitivity increase for ^{15}N observation. During the second (last) year of this grant, a new instrument design was initiated. Several studies were begun to elucidate the nature of chlorophenol interactions in liquids, and when incorporated into lecithin bilayer membrane models. Variable frequency ^{13}C spin lattice relaxation time (T$_1$) measurements were used to probe cooperativity of molecular chain dynamics in some simple molecules and in two complex synthetic polymers. A new theoretical modification involving a non-exponential autocorrelation function and also allowing for multiple independent internal rotations, allowed effective analysis of a large experimental set.

17. KEY WORDS AND DOCUMENT ANALYSIS

a. DESCRIPTORS	b. IDENTIFIERS/OPEN ENDED TERMS	c. COSATI Field/Group
Fourier analysis Fourier transformation Nuclear magnetic resonance toxicity biomathematics biomedical measurement		06 B, T

18. DISTRIBUTION STATEMENT RELEASE TO PUBLIC	19. SECURITY CLASS (This Report) UNCLASSIFIED	21. NO. OF PAGES 96
	20. SECURITY CLASS (This page) UNCLASSIFIED	22. PRICE PC A05 / MF A01

EPA Form 2220-1 (9-73)

EPA-600/1-77-045
September 1977

HIGH SENSITIVITY FOURIER TRANSFORM NMR
Intermolecular Interactions Between Environmental Toxic Substances and Biological Macromolecules

by

George C. Levy
Department of Chemistry
The Florida State University
Tallahassee, Florida, 32306

Grant 803095

Project Officer
Nancy K. Wilson
Environmental Toxicology Division
Health Effects Research Laboratory
Research Triangle Park, North Carolina, 27711

U.S. ENVIRONMENTAL PROTECTION AGENCY
OFFICE OF RESEARCH AND DEVELOPMENT
HEALTH EFFECTS RESEARCH LABORATORY
RESEARCH TRIANGLE PARK, N.C. 27711

ia

DISCLAIMER

This report has been reviewed by the Health Effects Research Laboratory, U.S. Environmental Protection Agency, and approved for publication. Approval does not signify that the contents necessarity reflect the views and policies of the U.S. Environmental Protection Agency, nor does mention of trade names or commercial products constitute endorsement or recommendation for use.

FOREWORD

The many benefits of our modern, developing, industrial society are accompanied by certain hazards. Careful assessment of the relative risk of existing and new man-made environmental hazards is necessary for the establishment of sound regulatory policy. These regulations serve to enhance the quality of our environment in order to promote the public health and welfare and the productive capacity of our Nation's population.

The Health Effects Research Laboratory, Research Triangle Park conducts a coordinated environmental health research program in toxicology, epidemiology, and clinical studies using human volunteer subjects. These studies address problems in air pollution, non-ionizing radiation, environmental carcinogenesis and the toxicology of pesticides as well as other chemical pollutants. The Laboratory develops and revises air quality criteria documents on pollutants for which national ambient air quality standards exist or are proposed, provides the data for registration of new pesticides or proposed suspension of those already in use, conducts research on hazardous and toxic materials, and is preparing the health basis for non-ionizing radiation standards. Direct support to the regulatory function of the Agency is provided in the form of expert testimony and preparation of affidavits as well as expert advice to the Administrator to assure the adequacy of health care and surveillance of persons having suffered imminent and substantial endangerment of their health.

This report represents a research effort to extend and improve analytical methodology for the examination of interactions of organic pesticides and other toxic substances in environmental systems. The results of several studies of the basic molecular phenomena underlying the toxic effects of these substances are included in the report.

John H. Knelson, M.D.
Director,
Health Effects Research Laboratory

ABSTRACT

This project explored the feasibility of developing new techniques for evaluation of the effects of environmental toxic materials on complex biopolymer systems using high sensitivity Fourier transform nuclear magnetic resonance (nmr) spectroscopy. Commercial instrumentation available in 1974-75 did not possess adequate sensitivity, and thus one goal of this project was to increase spectral sensitivity, especially for ^{13}C and other nuclides having low magnetogyric ratios. Initially, modifications to an existing Bruker HX-270 spectrometer provided moderate improvements in sensitivity for ^{13}C and a substantial sensitivity increase for ^{15}N observation. During the second (last) year of this grant, a new instrument design was initiated. While the latter nmr spectrometer was not completed during the period of this grant, it was clear that the limits of ^{13}C, ^{15}N, and metal nuclide sensitivity could be extended by at least an order of magnitude over that available on typical spectrometers. Improvements were also made in techniques required to obtain spin-relaxation and other nmr data.

Several studies were begun to elucidate the nature of chlorophenol interactions in liquids, and when incorporated into lecithin bilayer membrane models. In the latter case pentachlorophenol was observed to bind to the C-2, C-3 carbon region of the fatty acid alkyl chains, increasing the mobility of these chain fragments considerably. Evaluation of chlorophenol interactions in solution showed the presence of both inter and intra-molecular hydrogen bonding, when chlorines were substituted ortho to the hydroxyl groups.

Variable frequency ^{13}C spin lattice relaxation time (T_1) measurements were used to probe cooperativity of molecular chain dynamics in some simple molecules and in two complex synthetic polymers. A new theoretical modification involving a non-exponential autocorrelation function and also allowing for multiple independent internal rotations, allowed effective analysis of a large experimental data set. Application of this new approach to the study of correlated or cooperative motional dynamics in complicated biosystems is underway. It is hoped that new insight will be obtained into the organization of biopolymers and possible disruptions of this organization by interaction with toxic materials.

A short project demonstrated that high field ^{13}C nmr spectroscopy can be used to analyze complex mixtures of polychlorinated

biphenyls rapidly without prior separation. Analyses so obtained are not directly competitive with separation analysis techniques. However, they do serve well for screening and semi-quantitative identification.

This report was submitted in fulfillment of Grant No. 803095 by the Florida State University under the sponsorship of the U.S. Environmental Protection Agency. This report covers the period Oct. 2, 1974 to Oct. 1, 1976 and work was completed April 30, 1977.

CONTENTS

Disclaimer ii
Foreword iii
Abstract iv
Contents vi
List of Abbreviations and Symbols vii
Acknowledgement ix
Introduction 1
- A. NMR SENSITIVITY IMPROVEMENT AND DESIGN OF MORE EFFICIENT T_1 EXPERIMENTS 2
  - A1. Improvements of Bruker HX-270 High Field Spectrometer 2
  - A2. Seminole Project 5
  - A3. Time Saving in ^{13}C Spin-Lattice Relaxation Measurements by Inversion-Recovery. A Fast Inversion-Recovery FT NMR Pulse Scheme 8
  - A4. Optimal Use of a Non-Linear Three Parameter Fitting Procedure for Analyzing Inversion-Recovery Measurements of Spin-Lattice Relaxation Times 12
  - A5. Use of a Modified DEFT Pulse Sequence in ^{13}C NMR: Dynamic Range Improvement for Relaxation Experiments and Dynamic NMR Measurements at High Resolution 17
- B. INTERMOLECULAR INTERACTIONS 30
  - B1. Chlorophenol Effects on Model Membranes: ESR Study 30
  - B2. Chlorophenol Effects on Model Membranes: ^{13}C NMR Study 32
  - B3. Variable Field NMR Experiments on Model Membranes 35
  - B4. Variable Field ^{13}C T_1 Studies of Complex Systems 36
- C. INTERACTIONS OF CHLORINATED PHENOLS: HYDROGEN BONDING 38
- D. ANALYSIS OF POLYCHLORINATED BIPHENYLS BY CARBON-13 NUCLEAR MAGNETIC RESONANCE SPECTROSCOPY 39
- E. CHAIN MOLECULAR DYNAMICS IN COMPLEX MOLECULES 44

CONCLUSIONS 83

LIST OF ABBREVIATIONS AND SYMBOLS

ABBREVIATIONS

cal -- calories
CMR -- carbon-13 Nuclear Magnetic Resonance
$Cr(acac)_3$ -- trisacetylacetonatochromium
DCP -- dichlorophenol
DEFT -- "Driven Equilibrium Fourier Transform"
DNMR -- Dynamic nmr
DPL -- Dipalmitoyl Phosphatidyl choline
EPR -- Electron Paramagnetic Resonance
ESR -- Electron Spin Resonance
FID -- Free Induction Decay
FIRFT -- Fast Inversion Recovery Fourier Transform Pulse Sequence
FT -- Fourier transform
glc -- gas-liquid chromatography
IRFT -- Inversion-recovery Fourier Transform Pulse Sequence
NOE -- Nuclear Overhauser Effect
NTCFT -- a software package for the Nicolet 1080 minicomputer series
PBMA -- Poly(n-butyl methacrylate)
PCB -- polychlorinated biphenyl
PCP -- pentachlorophenol
PHMA -- Poly(n-hexyl methacrylate)
ppm -- parts per million
PSFT -- progressive saturation Fourier Transform pulse sequence
quad -- quadrature
rf -- Radio Frequency
S:N -- Signal to Noise
SRFT -- Saturation-recovery Fourier Transform pulse sequence
SEMINOLE -- Sensitivity Enhanced Modular Instrument for Nuclei of Low Enrichment
TCP -- tetrachlorophenol
WLL -- collectively the motional dynamics theories of Wallach, Levine & London

SYMBOLS

$D_a, \ldots D_i$ -- rotational diffusion constants

D_o -- isotopic rotational diffusion constant

E_a -- energy of activation

γ -- gyromagnetic ratio

G -- Gauss

$G(\tau_c)$ -- probability density function

h -- Planck's constant

$\vec{H}_o$ -- the laboratory magnetic field

$J_i(\omega)$ -- spectral density functions

J_{H-H} -- Spin-Spin Coupling constant (^1H-^1H)

λ -- chemical exchanged rate

$\vec{M}_A$, $\vec{M}_B$, M_A, M_B -- magnetizations

M_z -- magnetization in the (z) longitudinal direction

$\vec{M}_A^{tr}$, $\vec{M}_B^{tr}$ -- transverse magnetic components

η -- η = NOEF = NOE-1 NOE-factor

NT_1 -- total # of protons attached to the carbon times the T_1 of that carbon

p -- characteristic distribution width (log-χ^2 distribution

S_τ -- amplitude of a line after some waiting time τ

S_∞ -- amplitude of a line at thermal equilibrium

τ -- waiting time between pulses

τ_o, τ_c -- correlation time for molecular tumbling

τ_D -- correlation time of conformation transitions

τ_g, τ_{int} -- correlation time for internal rotation

τ_{max} -- longest τ

T_1 -- Spin Lattice Relaxation Time

T_1^e -- electron-induced spin-lattice relaxation

$T_{1\rho}$ -- spin lattice relaxation time in the rotating frame

T_2 -- spin-spin relaxation time

ω -- frequency in rad sec^{-1}

ω_A, ω_B -- Larmor frequencies of nucleus A and B

ACKNOWLEDGMENTS

The author acknowledges the work of Drs. E. Edlund, T. Holak, I. R. Peat, J. Kowalewski, D. Axelson, and J. Hochmann, as well as Ms. Mary Pat Cordes, Mr. James M. Hewitt, and Mr. Robert Schwartz. The author is particularly grateful to Dr. Nancy K. Wilson and the staff of the Health Effects Research Laboratory for their help and encouragement.

INTRODUCTION

The various techniques of Fourier transform (FT) nuclear magnetic resonance (nmr) spectroscopy[1] which have been developed in recent years, have become a powerful analytical tool for the elucidation of structure and chemistry in complex molecular systems. Possible applications[2] to environmentally significant problems have expanded at a rate proportional to improvements in nmr methodology and instrumentation.

The objectives of this research project were twofold. The first set of objectives sought to extend nmr spectroscopy sensitivity limits in order to make this technique more emenable to studies of complicated biosystems. The second set of objectives included initiation of a group of studies of environmental toxic materials and their chemical interactions with biosystems. Included in this work was evaluation of the interactions of chlorinated hydrocarbon, chlorophenol pesticides, and toxic heavy metals with phospholipid model cell membrane systems. In addition, studies of biological conformations were initiated for several peptide hormone systems (in collaboration with the National Research Council of Canada, Drs. I. C. P. Smith and R. Deslauriers).

While several of the initial objectives of this 2-year project were not fully realized, several unforeseen major developments occurred. These included:

(1) Initial design and construction stages of a new ultra-high sensitivity FT nmr spectrometer system, designed to extend present day sensitivity limits for environmentally significant studies of ^{13}C, ^{15}N, ^{31}P, and other nuclides under conditions approaching natural environmental sampling.

(2) NMR Studies of the chemically unique and biologically significant nitrogen nucleus ^{15}N at its natural isotopic abundance. This work has set boundary conditions for future applications. Included was development of ^{15}N nmr spin-labeling techniques which may become capable of resolving questions of biopolymer-toxin interactions for a class of toxins including several heavy metals (e.g., Mn, Cu, Fe, and lanthanide and actinide metals, etc.) as well as stable organic free radicals.

(3) The demonstration in our laboratory that ^{13}C T_1 data obtained at more than one magnetic field can be a unique and sensitive probe of transient higher structure in complex molecular

---

(1) Shaw, "Fourier Transform N.M.R. Spectroscopy", Elsevier (New York) 1976.

(2) R. Haque and F. J. Biros, eds. "Mass Spectrometry and NMR Spectroscopy in Pesticide Chemistry", Plenum (New York) 1974.

systems. Initial experiments indicate promise for application to studies of interrupted biofunction induced by toxin chemical interactions.

A. NMR SENSITIVITY IMPROVEMENT AND DESIGN OF MORE EFFICIENT T_1 EXPERIMENTS

A1. Improvements of Bruker HX-270 High Field Spectrometer.

When our Bruker HX-270 spectrometer was installed we had ^{13}C and ^{15}N sensitivity which was only 25%-30% better than that available on a 1973 stock Varian XL-100 spectrometer. Combining the various methods discussed immediately below, we have been able to obtain a factor of >3 improvement in ^{13}C and ^{15}N sensitivity.

It is important to note that these improvements are stated in terms of signal-to-noise (S:N), the decrease in time requirement is a factor of 10 for ^{13}C and over 50 for ^{15}N. Thus we have been able to perform experiments that are impractical on typical FT nmr systems. One application for our improved sensitivity is the ^{13}C T_1 study of model membranes (Section B) underway. Another application is the use of ^{15}N nmr for spin-labeling experiments. Here we are beginning to take advantage of the chemical specificity of nitrogen to probe interactions of paramagnetic toxic heavy metals with biological molecules.

Table 1 summarizes the ^{13}C sensitivity of our Bruker HX-270 as developments were added.

TABLE 1.

FSU BRUKER HX-270 CHRONOLOGY

YEAR	IMPROVEMENT	RESULTING S:N[a]
1973	--	75(10mm tubes)
1974	decoupler	90(10mm tubes)
1975	quadrature detection	120(10mm tubes)[b]
1975	larger sample probes	225(13mm tubes)[c]
1976	larger sample probes	~300(15mm tubes)[d]

[a] Standard test 50% ethyl benzene, single 90° pulse, 15kHz spectral window, ca. 0.8 Hz line broadening applied;

[b] 2ml required;

[c] 3.5ml required;

[d] 5.0ml required.

The actual S:N numbers in Table 1 are not relevant. The HX-270 spectrometer does not achieve the best results on a narrow line spectrum such as that for ethyl benzene, due to decoupler and lineshape limitations that have never been fully analyzed. A sample which we use for evaluation of sensitivity is 1.0M sucrose in H_2O/D_2O. A typical single pulse spectrum of 1.0M sucrose is given in Figure 1. The observed S:N is 25:1.

Figure 2 shows a typical ^{15}N sensitivity check. The spectrum shown was obtained with a single 90° pulse.

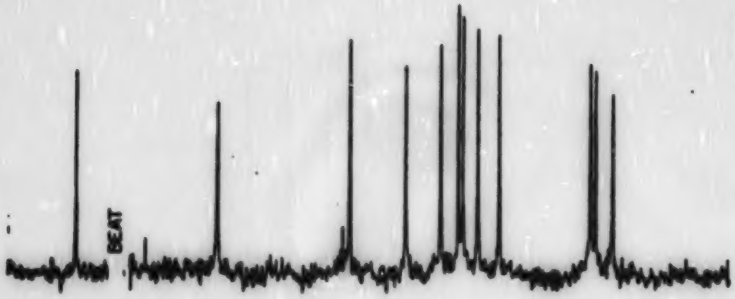

FIGURE 1. ^{13}C Sensitivity of the FSU HX-270 (15 mm sample).

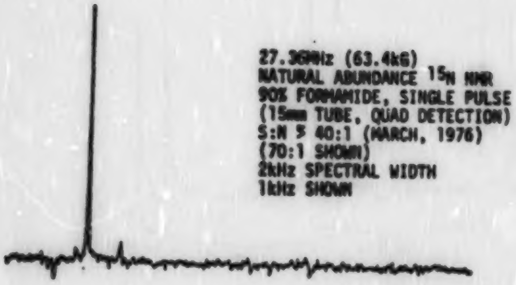
27.36MHz (63.4kG)
NATURAL ABUNDANCE ^{15}N NMR
90% FORMAMIDE, SINGLE PULSE
(15mm TUBE, QUAD DETECTION)
S:N ≥ 40:1 (MARCH, 1976)
(70:1 SHOWN)
2kHz SPECTRAL WIDTH
1kHz SHOWN

FIGURE 2. ^{15}N Sensitivity of the HX-270, 15 mm sample.

Figure 3 shows that ^{15}N T_1's can be determined efficiently on our HX-270 spectrometer. This entire T_1 and nuclear overhouse effect (NOE) experiment (shown for a neat sample in a 13mm tube) was run in less than 1 hour. This experiment simultaneously measures T_1's and NOE's. (In section A3 we will show further efficiency improvements in ^{15}N T_1 measurements).

One final ^{15}N spectrum is shown below (Figure 4). This is a natural abundance coupled spectrum of formamide.

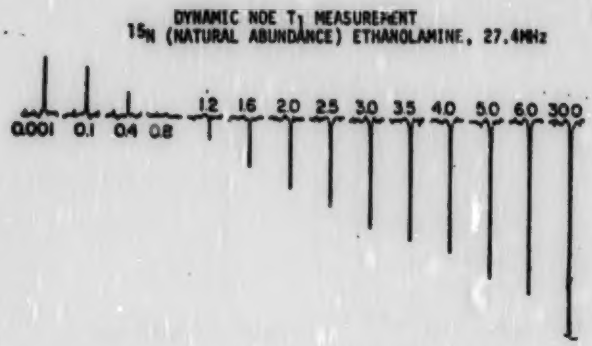

FIGURE 3. Dynamic NOE T_1 and NOE Measurement: ^{15}N, 27.4 MHz, neat ethanolamine.

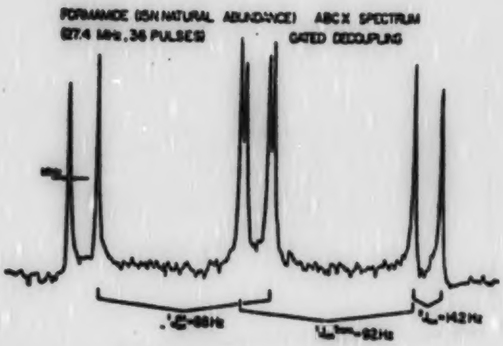

FIGURE 4. Undecoupled ^{15}N Spectrum of Formamide, 36 scans, gated decoupling.

A2. Seminole Project.

In our EPA proposal we planned to up-date and optimize our HFX-90 spectrometer. For several reasons we decided to abandon that course. The HFX-90 magnet and console are now 11 years old and are showing signs of wear with respect to reliability.

Furthermore, we realized that our narrow gap 21kG magnet would never be sufficient for sensitivity improvements beyond 15mm sample tubes. Thus, after modifying the HFX-90 as much as possible (to include quadrature detection), we embarked on design and construction of an entirely new spectrometer, names tne SEMINOLE [Sensitivity Enhanced Modular Instrument for Nuclei Of Low Enrichment]. The SEMINOLE will be a large sample, intermediate field superconducting solenoid-based spectrometer, designed to observe any nuclide having a magnetogyric ratio below that of ^{205}Tl.

The SEMINOLE spectrometer will be ideally suited for a number of environmental studies where large samples are available:

1. ^{13}C Analysis of organic compounds in natural and processed drinking waters.
2. Speciation of phosphorus in interstitial and other waters.
3. Examination of interactions of environmental toxins with biosystems using ^{13}C, metal nuclei nmr, and ^{15}N spectroscopy (with enrichment).

Other applications of course are possible. Some examples are given in Section B.

Progress on the SEMINOLE has been fairly good over the past six months.

We are currently operating with 20, 25, and 30mm sample tubes at a field of 21kG (22.63MHz for ^{13}C). The final operating field for the SEMINOLE will be 35kG, corresponding to 150MHz for ^{1}H. We will initiate operation at 35kG in early May 1977.(*)

Some early 21kG test spectra for the SEMINOLE are shown below. The line-shape and resolution of the initial solenoid, while adequate for 25mm operation, was inadequate with 30mm sample tubes. The result was lower sensitivity than expected. Using our own 22.6MHz preamplifier and temporary 2MHz i.f. quad detection receiver we maintained ^{13}C sensitivity of ca. 150:1 on 50% ethyl benzene versus 300 to 500:1 as would be desirable prior to probe re-design.

(*) After set-up of a replacement magnet by Bruker. The initial SEMINOLE magnet, while performing reasonably well, had not met specifications.

Figure 5 shows a single pulse spectrum for CS_2 with 0.4Hz resolution in a 30mm sample tube. Spinning sidebands are 3-6% generally.

Figure 6 shows a 30mm sample of dioxane with 3 watts of wide-band ^1H decoupling. The resulting resolution of 0.8Hz with only 2% spinning sidebands is rather difficult to achieve on our current magnet.

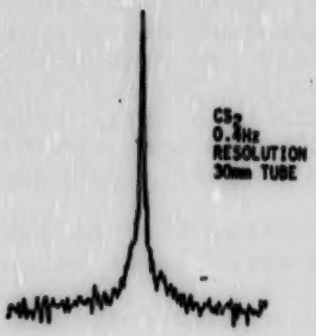

FIGURE 5. 30 mm Sample of CS_2 showing resolution of 0.4 Hz.

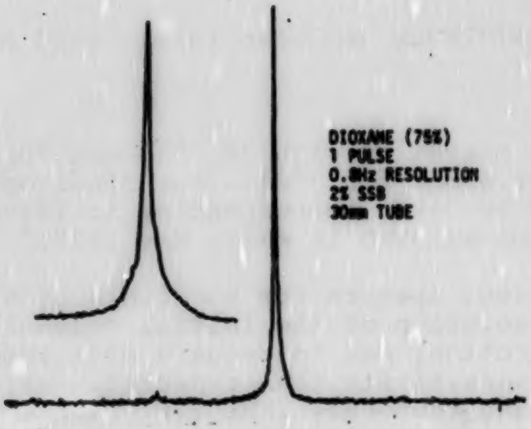

FIGURE 6. 30 mm Sample of dioxane showing 0.8 Hz resolution.

One outstanding feature of the SEMINOLE is its H_1 rf homogeneity for intermediate and large sized samples. Figure 7 shows an excellent signal for a 15mm x 15mm cylindrical sample. In 30mm samples we are still able to achieve ratios of >10:1 for 90° versus 180° pulses. This contrasts with ≳3 or 4:1 for only a 10mm sample in a Bruker HX-270 spectrometer.

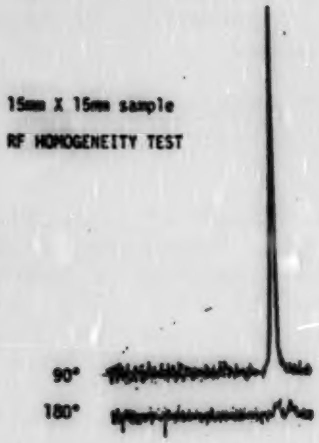

FIGURE 7. Rf Homogeneity Test. 90° and 180° pulse response from a 15 mm 415 mm cylindrical sample.

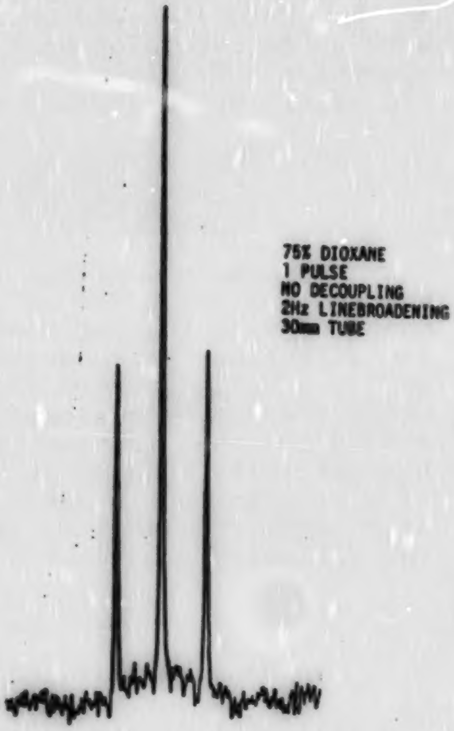

FIGURE 8. Single 90° pulse on 75% dioxane, undecoupled, 30 mm sample.

One other SEMINOLE test spectrum is shown in Figure 8. This is a single pulse coupled (no NOE) spectrum of 75% dioxane. The sensitivity here is not poor but we feel that we can do considerably better with improvements now underway in the preamplifier and probe. The new solenoid and operation at 35kG should give an improvement a factor of ca. 3 in signal-to-noise for small molecules.

In considering the design of the SEMINOLE we are attempting to partially circumvent two limitations of the highest sensitivity spectrometer developed to date, the Bruker WH-180:

1. Decreased ^1H decoupling efficiency for large samples at 180MHz
2. High field spin-lattice relaxation disadvantages for biopolymer studies.

The somewhat lower final operating field of the SEMINOLE (relative to the WH-180) should prove to be a good compromise for biopolymer work while retaining most of the inherent sensitivity of high field operation. We are constructing an especially powerful ^1H decoupler (80 watts, up to 20gauss for large sample tubes)

A3. Time Saving in ^{13}C Spin-Lattice Relaxation Measurements by Inversion-Recovery. A Fast Inversion-Recovery FT NMR Pulse Scheme.

Measurements of spin-lattice relaxation times in multiline NMR spectra are often achieved by the inversion-recovery method combined with Fourier transform (IRFT).[3] This method is based on the well-known pulse sequence: $[180°-\tau-90°(FID)-T]_n$. T is a time set to $5(T_1)_{max}$, where $(T_1)_{max}$ is the longest spin-lattice relaxation time to be measured. The free induction decays (FID's) are stored and then Fourier transformed leading to a spectrum which has partially relaxed for a time, τ. If we call S_τ the amplitude of a line in such a spectrum and S_∞ the corresponding amplitude at thermal equilibrium, the relaxation time T_1 can be deduced from the following equation:

$$S_\tau = S_\infty[1 - 2\exp(-\tau/T_1)]. \qquad (1)$$

The applicability of this method is limited by the duration of the experiment which depends on the number of scans, n, and on the waiting time, T. This difficulty is particularly severe for low sensitivity nuclei wuch as ^{13}C (or ^{15}N) because these nuclei may have long relaxation times and because extensive time averaging may be required even to obtain a single spectrum. The problem becomes less acute with methods based on 90° pulse sequences which do not utilize a long waiting time (so-called saturation-recovery sequences, SRFT). These sequences can be obtained using a burst of 90° pulses[4] or by field inhomogeneity gradients.[5] A similar result to eliminate magnetization [cause saturation]is more simply obtained by progressive saturation (PSFT),

---

(3) R. L. Vold, J. S. Waugh, M. P. Klein, and D. E. Phelps, J. Chem. Phys., **48**, 3831 (1968).

(4) J. L. Markley, W. H. Horsley, and M. P. Klein, J. Chem. Phys., **55**, 3604 (1971).

(5) G. G. McDonald and J. S. Leigh, Jr., J. Magn. Resonance, **9**, 358, (1973).

as proposed by Freeman and Hill.[6,7] These authors showed that sequences of the type: $[90\text{-(FID)-}\tau]_n$ lead to spectra obeying Eq. (2).

$$S_\tau = S_\infty[1 - \exp(-\tau/T_1]. \tag{2}$$

However these three rapid methods entail a loss of dynamic range (or sensitivity) of 50% with respect to inversion recovery. Furthermore, they require minor instrumental adaptations. The PSFT method is also not appropriate for short relaxation times, because data acquisition and resolution requirements place a lower limit on τ.

We wish to show here that inversion-recovery with an arbitrary short waiting time is comparable to the SRFT and PSFT methods in speed, and that such a sequence gives optimum dynamic range with respect to experimental time for each individual resonance line. (For a set of T_1 spectra, dynamic range is essentially equivalent to sensitivity[6,7,8]). Furthermore, this new sequence does not share many of the disadvantages of the SRFT and PSFT sequences.

In this case we observe three "short" T_1's and one "long" T_1. The FIRFT sequence gains an advantage over the SRFT and IRFT methods when there is a range of T_1's to be determined, including T_1's ≥ 10 sec. When all T_1's to be determined in a spectrum are very long and approximately equal, then the FIRFT and SRFT sequence are comparable in efficiency.

TABLE 2.

COMPARISON OF IRFT AND FIRFT EXPERIMENTS.
80% (w/v) PHENOL IN D_2O[a]

CARBON	T_1(seconds)[b] IRFT[c]	FIRFT[d]
C-1	29.5	28.8
C-2	4.2	4.2
C-3	4.1	4.0
C-4	3.1	3.0

---

(6) R. Freeman and H. D. W. Hill, J. Chem. Phys., 54, 3367 (1971).

(7) R. Freeman, H. D. W. Hill and R. Kaptein, J. Magn. Resonance, 7, 82 (1972).

(8) G. C. Levy and I. R. Peat, J. Magn. Resonance, **18**, 500 (1975).

[a] T_1's determined at 67.9MHz and 40°C; sample not degassed.

[b] The accuracy of these T_1's is ±5% (2 standard deviations).

[c] $(T-180°-\tau-90°)_5$: T=5 sec; τ values, 0.05, 0.5 1.0, 1.5, 2.0, 2.5, 3.0, 4.0, 5.0, 10.0, 20.0, 30.0, 40.0, 160.0.

[d] $(T-180°-\tau-90°)_5$: T=160 sec; same τ values.

We called this method[9] fast inversion recovery (FIRFT) by contrast to standard inversion recovery (IRFT). The sequence utilizes a waiting time T much smaller than $5(T_1)_{max}$ but sufficient to allow the decay of transverse magnetization before the next 180° pulse. This is actually achieved in a short time for carbon-13 measurements with broad-band proton irradiation. The successive FID's have amplitudes equal to:

$$S_\infty[1 - 2\exp(-\tau/T_1)];\ S_\infty[1 - (2 - E_1)\exp(-\tau/T_1)];\ldots;$$

$$S_\infty[1 - (2 - E_1)\exp(-\tau/T_1)],\ \text{where } E_1 = \exp(-T/T_1). \qquad (3)$$

The accumulated signal S_τ is consequently related to:

$$S_\tau = S_\infty[1 - \alpha\exp(-\tau/T_1)] \qquad (4)$$

with

$$\alpha = (2 - E_1)[(n - 1)/n)]. \qquad (5)$$

If n is large or if the first FID is deleted S_τ reduces to:

$$S_\tau = S_\infty[1 - (2 - E_1)\exp(-\tau/T_1)] \qquad (6)$$

and the usual logarithmic plot* allows the determination of T_1:

$$\ln(S_\infty - S_\tau)/S_\infty) = \ln\alpha - \tau/T_1. \qquad (7)$$

τ values are chosen exactly as in a conventional IRFT experiment. Of course,the measurement of S_∞ requires that one spectrum be obtained where τ is $\geq 5(T_1)_{max}$. If exponential fits are used, even this requirement is waived (see section A4).

Note from Eq. (6) that instead of a dynamic range of 2 as in the standard IRFT sequence, the FIRFT sequence has a dynamic range of $(2 - E_1)$, where $E_1 < 1$. The dynamic range or overall sensitivity

(9) D. Canet, G. C. Levy, and I. R. Peat, J. Magn. Resonance, **18**, 199 (1975).

*Standard automated calculations can be used without modification; only the intercept is altered.

of the experiment is optimized for each resonance line since E_1 is very small when the waiting period, T, is longer than or comparable to T_1. When $T<<T_1$, E_1 approaches 1 and the dynamic range is reduced to that of the SRFT and PSFT methods.

Thus the dynamic range will vary from a little over 1 (for very long T_1's) to exactly 2 (for very short T_1's) for different nuclei during a single experiment, whose total experimental time can be up to an order of magnitude shorter than with the standard IRFT sequence. The exact time saved depends on the discretionary value of T in both cases (e.g., 3 to 5 times T_1 in IRFT; 1 to ca. 10 sec in FIRFT) and on the number of scans, since the IRFT does not discard the first FID.

Figure 9 and Table 2 show the results of conventional IRFT and FIRFT experiments on a solution of 80% (w/v) phenol in D_2O. The factor of 7 in time savings for the FIRFT experiment (see Table 2) is, of course, partly offset by the increase in dynamic range of the IRFT experiment. (Note that for the protonated carbons the FIRFT dynamic range is nearly as large as in the conventional IRFT experiment). Also, in the IRFT scheme a reduction in the waiting time, T, to $4(T_1)_{max}$ would lower the FIRFT time advantage by ca. 20%.

(a) FIRFT EXPERIMENT

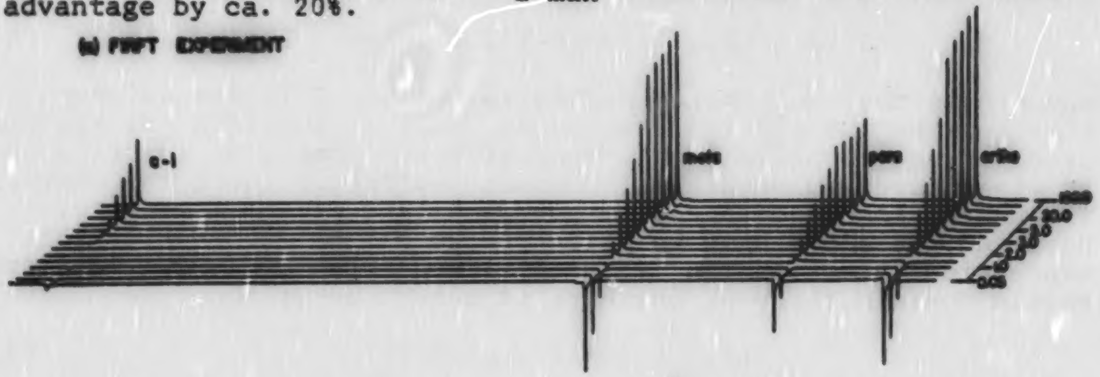

(b) CONVENTIONAL IRFT EXPERIMENT

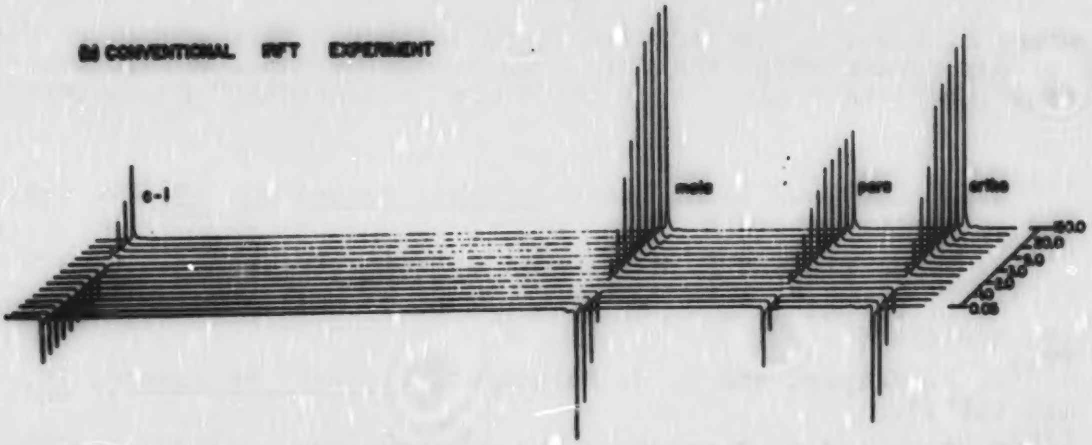

FIGURE 9. Comparison of IRFT and FIRFT pulse sequences for a sample of phenol in D_2O.

A4. Optimal Use of a Non-Linear Three Parameter Fitting Procedure for Analyzing Inversion-Recovery Measurements of Spin-Lattice Relaxation Times.

In recent years the methodology for accurate measurements of nuclear spin-lattice relaxation times (T_1's) has occupied the attention of many authors. In particular, choices of pulse sequence[10,11], delay times[11,9] and data reduction methods[12-14] have been discussed extensively.

In an earlier communication from this laboratory[9], we advocated use of the inversion-recovery method with a short waiting time, T, between pulse sequences (fast inversion-recovery, FIRFT). This method has the advantage of speed while also retaining the advantage of maximum available or optimized dynamic range. As has been pointed out[12-14], the determination of T_1's can further be shortened by omitting the time consuming measurement of the equilibrium magnetization corresponding to $\tau > 5T_1$ in the $(180°\text{-}\tau\text{-}90°\text{-}\underline{T})_n$ sequence. In order to obtain this additional time saving, it is, however, necessary to replace the usual semi-logarithmic plot method of data reduction by a non-linear least squares fitting procedure. For an ideal experimental case, the signal intensities may be fitted to a two-parameter expression:

$$S(\tau) = A[1-2(1-\exp(-\underline{T}/T_1))]\exp(-\tau/T_1) \qquad (8)$$

where A is the equilibrium magnetization and T is the waiting time between the $180°\text{-}\tau\text{-}90°$ sequences. Use of equation (8) has the disadvantage of being highly sensitive to systematic errors such as misadjusted pulse angles, frequency offset between the carrier frequency, the resonance line positions and rf inhomogeneity. Sass and Ziessow[14] have recently suggested that a more flexible expression to which the measured signal intensities can be fitted should contain three parameters, it should be of the type:

$$S(\tau) = A + B\exp(-\tau/T_1) \qquad (9)$$

where A, B and T_1 are adjustable parameters. This procedure does not overparameterize the data. In fact, the usual method using semi-logarithmic plots contains three "independent" parameters:

---

(10) G. C. Levy and I. R. Peat, J. Magn. Resonance, 18, 500 (1975) and references therein.

(11) R. K. Harris and R. H. Newman, J. Magn. Resonance, 24, 449 (1976).

(12) D. L. DeFontaine, D. K. Ross and B. Ternai, J. Magn. Resonance, 18, 276 (1975).

(13) T. K. Keipert and D. W. Marquardt, J. Magn. Resonance, 24, 181 (1976).

(14) M. Sass and D. Ziessow, J. Magn. Resonance, 25, 263 (1977).

(1) the equilibrium magnetization (which is fixed and in general rather accurately determined), (2) the slope and (3) the intercept of the best straight line. Deviations from experimental ideality in semilogarithmic plots show up first in the intercept of the line. Since T_1 is calculated from the slope of this line and not the intercept, T_1 is relatively insensitive to pulse and mild frequency offset defects in IRFT[10] and FIRFT[9] experiments. Sass and Ziessow[14] have shown that the non-linear three parameter fit procedure is capable of producing *reliable* data in cases of misadjusted pulses and for large frequency offsets.

In this discussion we present a simple and empirical attempt to find the minimal acceptable value for the longest $\tau(\tau_{max})$ used in FIRFT experiments. We also discuss some additional ramifications of the use of exponential fitting procedures for T_1 determination.

The results of three experiments using different waiting times, *T*, are presented in Table 3. The error limits quoted in the table are standard deviations.[15] The most important feature of these results is the great increase of the uncertainty (measured by large standard deviations) for τ_{max} of order of T_1 or less. This decreased accuracy is only to a minor extent due to a small number of experimental points, as can be seen in the comparison of two sets of data using 8 τ's covering different ranges (calculations 2 and 8, Table 3.) (It is *important* to realize that the 8 calculations were performed on the same 3 experimental data sets.) Rather, the loss of accuracy is due to the fact that excluding longer τ's makes the function of eq. 9 less well-defined, greatly increasing the correlation between parameters. This is illustrated in Figure 10, for the cases of T=1.5 sec and eight experimental points covering a "small" and "large" range of τ's (calculations 2 and 8). The figure presents the variance (sum of squared errors divided by number of degrees of freedom) corresponding to adjustment of parameters A and B, eq. 9 at fixed T_1 versus these T_1 values. The sharpness of the minimum is a significant measure of accuracy: the T_1 range corresponding to a doubling of the minimum variance may be used as a realistic estimate of possible calculated T_1 error limits. For the case of the large τ value range, calculation 2, the limits are about ±2.5%. For calculation 8, including τ values only up to *ca.* 0.8 T_1, gives an error limit exceeding ±10%. Figure 1 shows that calculation 8 gives a T_1 that is too low and furthermore well outside of the error limits for calculation 2. On this basis only, it appears necessary to use τ values covering a range up to at least 1.5 or 2 T_1 for *accurate* determination of T_1's. Inclusion of such τ's is also motivated by dynamic range and signal-to-noise considerations, since the peak intensities may be rather attenuated for

---

(15) As calculated according to standard practice; see for example W. E. Deming, "Statistical Adjustment of Data," John Wiley & Sons (New York) 1943.

short τ values in the FIRFT experiment (when the ratio $\underline{T}/T_1$ is small).

A few other comments might be made concerning the calculations shown in Table 3:

1. For these experiments, no significant increase in accuracy was noted with larger numbers of τ values. Only the *range* of τ values covered affected the precision and accuracy of the T_1 calculation.

2. As long as one or more "long" τ values were included in the data set, there was no significant loss in accuracy for the three experimental values of $\underline{T}$. Since the time $\underline{T}$ is required to obtain each τ value, it is far more efficient to use a shorter $\underline{T}$ and one or two long τ values as in experiment 3 calculation 2, than to utilize long $\underline{T}$ values as in experiment 1 (approaching a normal IRFT experiment). Note however that for experiments where signal-to-noise ratios are low and T_1's are long, the use of a short $\underline{T}$ will negate the use of short τ values since the signals will then be below the noise level. In this case, well spaced τ values starting at a low value and including several τ's of the order of the estimated T_1 will produce optimum results.

3. Use of the exponential fit for determination of T_1 circumvents a systematic problem inherent in semi-logarithmic plots, that is, biased error limits.[10]

The data shown in Table 3 and Figure 10 have been obtained using the general least-squares program GENLSS[16] on an off-line CDC6400 computer. For routine purposes, when elaborate statistical analysis is not necessary, the least squares fitting may also be performed using on-line minicomputers. This procedure greatly reduces the effort needed for evaluation of the T_1 data and it is being extensively used in this laboratory. We are utilizing a modified version of the NTCFT software package, available for Nicolet 1080 series minicomputers.

Unmodified NTCFT softward currently contains a two parameter exponential fit T_1 calculation using eq. 8 that works only under near-ideal experimental conditions. Our 3-parameter fit calculation[17] was successfully used for a large number of experiments including cases where mis-set pulse angles and large frequency offsets were intentionally introduced. In all cases the 3-parameter fit calculated on the Nicolet computer was equivalent or superior to semi-logarithmic data treatment. Our current on-line

---

(16) D. F. DeTar, "Computer Programs for Chemistry," Vol. IV, Academic Press (New York), 1972.

(17) Available from the authors and recently added to the product line by Nicolet Technology.

3-parameter fit, however, is not extremely time efficient. Typical T_1 calculations require 1-3 min. but can take considerably longer if the data set is poor (e.g., low signal-to-noise and poor choice of τ values).

TABLE 3. PROTON T_1's OF 2% ACETONE SOLUTION IN $CDCl_3$.[a]

	Characteristics of τ Values Used in the Fitting Procedure		Calculated T_1 (sec)		
Calculation	τ_{max} (sec)	Number of τ's	Experiment 1 W = 17 sec	Experiment 2 W = 6 sec	Experiment 3 W = 1.5 sec
1	17	18	5.25±.06	5.35±.05	5.21±.05
2	17	8	5.21±.03	5.33±.05	5.19±.06
3	11	17	5.42±.08	5.40±.07	5.23±.07
4	8	16	5.23±.07	5.39±.10	5.14±.09
5	7	14	5.27±.08	5.25±.12	5.01±.11
6	6	12	5.21±.11	5.25±.12	4.92±.15
7	5	10	5.11±.16	5.45±.19	4.74±.17
8	4	8	5.07±.27	5.32±.31	4.99±.24

[a] At 270 MHz and 30°C; solution not degassed.

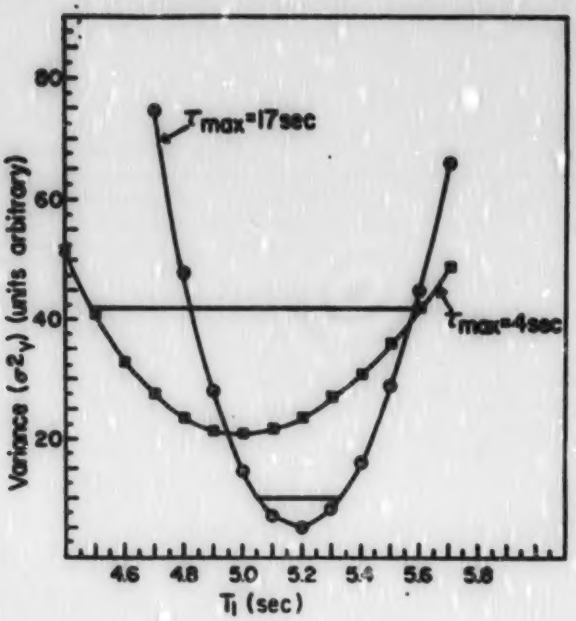

Figure 10. The variance corresponding to least-squares adjustment of A and B using eq. (2) as a function of a fixed T_1. Eight experimental points have been used, the τ's were the same as in calculations 2 (●) and 8 (■). (See Table 3).

A5. Use of a Modified DEFT Pulse Sequence in ^{13}C NMR: Dynamic Range Improvement for Relaxation Experiments and Dynamic NMR Measurements at High Resolution.

Introduction

A refocusing three pulse sequence, "Driven Equilibrium Fourier Transform" (DEFT), was introduced in 1969[18]. The stated application for DEFT was signal enhancement in situations where nuclear spin-lattice relaxation times (T_1's) were too long to allow rapid repetition of scans in normal FT nmr spectroscopy. As a result of experimental difficulties,[19] the DEFT sequence has not been widely applied to high resolution nmr spectroscopy. We describe here an application of a variation[20] of the DEFT ($90°-\tau-180°-\tau-90°-T)_n$ pulse scheme which is useful, not for signal enhancement but for effective suppression of single or multiple large solvent lines in nmr spectra, even during T_1 determinations. A second, and unrelated, application to be described, involves measurement of dynamic nmr (DNMR) parameters, i.e., chemical exchange rates.

The first application, peak suppression, can be easily performed on typical commercial spectrometers. Required rf homogeneity and other stringent experimental conditions limit applicability of this sequence for DNMR studies.

In reference 20 a significant simplification of the ^{1}H-spectrum of a large paramagnetic protein was achieved through the application of the "Modified DEFT" pulse-sequence [$90°-\tau-180°-\tau-90°$ data acquisition]. The modification derives from the fact that the data are acquired after the final 90°-pulse, and not during the waiting period between pulses, as in the usual DEFT-technique. For every resonance having $T_1>\tau$, the longitudinal magnetization M_z, built up during the first waiting period τ, is approximately τ/T_1. The 180° pulse inverts M_z, and then during the second period τ-M_z is eliminated to second order in (τ/T_1). The signal resulting after the final 90°-pulse is then roughly proportional to $(\tau/T_1)^2$, which supplies effective suppression for resonances where τ/T_1 is less than ca. 0.13. Resonances having $T_1 \approx \tau$ or $T_1<\tau$ provide signals following the equation:

$$S_\tau = S_\infty \left[1-2\exp(-\tau/T_1) + (1-a)\exp(-2\tau/T_1)\right] \qquad (10)$$

where S_τ is the measured resonance amplitude, $S_\infty = S(\tau=\infty)$, T_1 is the spin-lattice relaxation time, and a accounts for pulse-imper-

---

(18) E. D. Becker, J. A. Ferretti, and T. C. Farrar, J. Am. Chem. Soc., 91, 7784 (1969).

(19) R. Freeman and H. D. W. Hill, J. Magn. Resonance, 4, 336,(1971).

(20) J. Hochmann and H. P. Kellerhals, J. Magn. Resonance, to be submitted.

fections (c.f. reference 20). The principal advantage of this technique is the possibility of measuring T_1's of fast relaxing lines by the variation of τ over an appropriate range and fitting of the resultant signals to equation 10, at the same time suppressing *all* slowly relaxing lines (even if those lines have quite different T_1's). The degree of suppression achievable, *ca.* 10^2, is less than that obtainable by other peak-peak suppression methods.[21-22] However, the other methods cannot extend peak suppression over a reasonable range of τ values, nor do they operate for multiple lines having significantly different T_1's. The present method deals with the dynamic range problem encountered commonly in ^{1}H nmr, or in ^{13}C-T_1 measurements when dilute solutions are utilized and the solvent contains carbon.

Experimental

The measurements were performed on our spectrometer SEMINOLE, based on a wide bore superconducting solenoid, and currently operating at the ^{13}C frequency of 22.63 MHz. Quadrature-detection at an i.f. of 2.05 MHz was used for these experiments. Pulse timing was obtained with a Nicolet 293 universal controller. The probe uses a single 4 turn Helmholtz-coil (diameter 35mm, height 35mm). All spectra were recorded with broadband proton decoupling. The temperature was controlled with an input thermocouple-regulated temperature controller. For the peak suppression experiment a 30mm spinning tube (height of sample, 50mm) was used. It contained 0.4M of commercial reagent grade cholesteryl chloride in cyclohexane (10% cyclohexane-d_{12}).

With the 30mm tube the solvent line is ≈100 times stronger than the individual steroid resonances (Figure 11). The strong (effectively, ≈50M) solvent signal in this large sample exceeds the linear range of the *receiver* giving rise to the baseline artifacts (see Figures 11a and 12a). For chemical exchange applications of the modified DEFT sequence, experimental requirements are far more stringent than for peak suppression experiments. The DNMR experiments in principle differ from the peak suppression experiments only by using τ spacings in the 1-25 msec range (of the same order as the chemical exchange lifetime). In fact, r.f. homogeneity and other instrumental requirements for the DNMR experiment described below are only marginally met with our spectrometer, such that a smaller 15mm sample, a very narrow spectral window, *and* a specific choice of τ were required to achieve a 1% null for the non-exchanging acetyl methyl carbon (see the discussion below.) Deviations from this choice of τ, use of a larger

(21) A. G. Redfield, S. D. Kunz, and E. K. Ralph, *J. Magn. Resonance*, **19**, 114 (1975); J. P. Jesson, P. Meakin, and G. Kneissen, *J. Am. Chem. Soc.*, **95**, 618 (1973).

(22) S. L. Patt and B. D. Sykes, *J. Chem. Phys.*, **56**, 3182 (1972). F. W. Benz, J. Feeney, G. C. K. Roberts, *J. Magn. Resonance*, **8**, 114 (1972)

sample or larger spectral offset, or inclusion of sample spinning individually resolted in DEFT "null" signals of 5 to >10% for the acetyl methyl carbon.

T_1 Determination Using the Modified DEFT Sequence

In the steroid sample, T_1 for cyclohexane is about 15 sec; T_1's of the steroid lines range from 0.4 to 5 sec. This difference enabled us to achieve a T_1 measurement on nearly all carbons of the steroid with simultaneous suppression of the solvent line by the Modified DEFT sequence. Calculation of T_1 values from the data using equation (10) was performed with the general least squares program GENLSS.[16]

As can be seen in Figures 11c and 12b, the solvent resonance can be suppressed effectively with the Modified DEFT-sequence for τ-values of about 1 sec, in agreement with the theoretical prediction of $\sim(T_1/\tau)^2$. For shorter τ's, however, which become comparable with T_2 of the solvent-line, the suppression factor is lower, typically *ca.* 20, due to imperfect nulling of the residual transverse magnetization by the final 90° pulse, (using a 30mm spinning tube with corresponding limited r.f. homogeneity). We plan to circumvent this problem by the use of a homospoil pulse.

Table 4 contains resulting T_1 values for six selected resonances of the steroid. In those cases where standard inversion-recovery T_1 data were obtainable (lines well separated from the solvent resonance), there was good agreement between the modified DEFT and IRFT determined T_1's.

TABLE 4. T_1 VALUES FOR SELECTED CARBONS OF CHOLESTERYL CHLORIDE[a]

Carbon	T_1(sec)[b,c] Inversion-Recovery	T_1(sec)[b,d] Modified DEFT
11	0.53	0.53
7,8 (unresolved)	0.63	0.64
3	0.87	0.85
27	1.84	1.88
9	0.94	0.90
6	0.90	0.93

(a) 0.4M in cyclohexane (10% d_{12}-cyclohexane), 41°C, 22.63MHz; (b) Estimated accuracy ±5-10%; (c) Calculated from $S(\tau)=S_\infty[1-a' \exp(-\tau/T_1)]$ using a three parameter non-linear least squares fit; (d) calculated from eq. 1, same method as in (c).

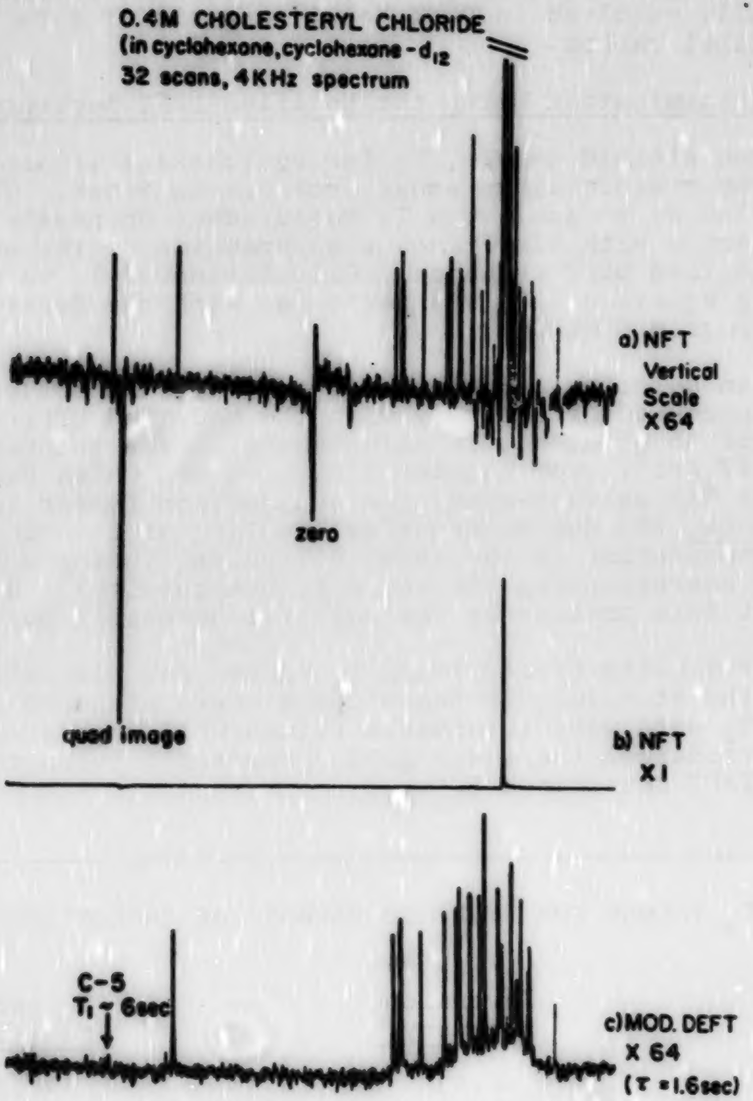

FIGURE 11. 22.63 MHz ^{13}C NMR Spectra of 0.4 M cholesteryl chloride in cyclohexane (10% cyclohexane d_{12}), 30mm sample, 41°C: (a) and (b) Normal FT spectrum, vertical scale expanded in (a); (c) modified DEFT spectrum. For both cases 32 scans were accumulated, with a pulse sequence interval of 80 sec. For the modified DEFT spectrum τ was 1.6 sec. The spectral width in each case is 4kHz. Baseline rise in Figure 1c results from H_0 inhomogeneity and not from the DEFT experiment.

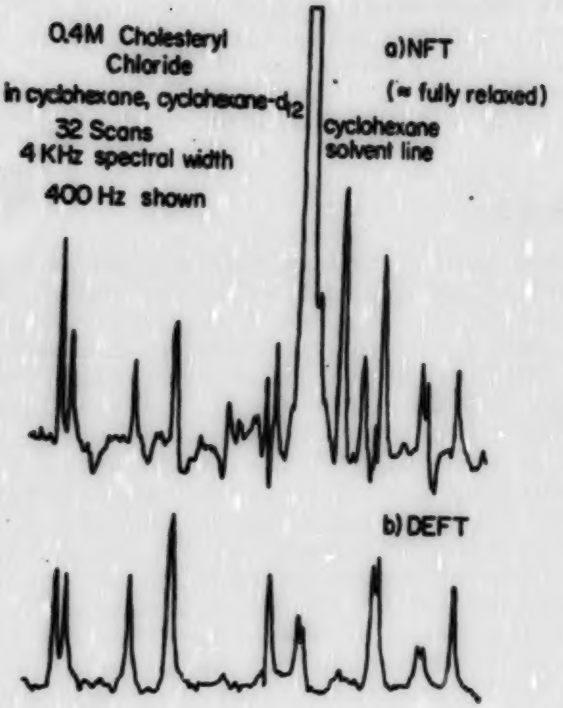

FIGURE 12. Spectral expansion of the data in Figures 11a and 11c. 400 Hz spectral width shown. (Use of 80 sec pulse interval emphasizes the cyclohexane-d_{12} resonances in Figure 12a). Harmonic and other baseline distortions are visible in Figure 12a.

Use of the modified DEFT scheme for T_1 determinations offers many practical advantages. In particular, the stringent experimental requirements necessary to the use of the normal DEFT technique are loosened. Nevertheless, it is possible to realize such conditions (mainly a good rf homogeneity) using small, nonspinning samples in our large receiver coil. This allows a relatively precise alignment of the nuclear magnetization with H_0 through the final 90° pulse of the DEFT-sequence and thus an effective zeroing of the transverse magnetization.* This stimulated our interest in a possible application of DEFT in Dynamic NMR (DNMR) at high resolution, based on the fact that the chemical exchanging resonances will not have their transverse components zeroed, due to exchange-induced dephasing during the two waiting periods, τ.

Chemical Exchange

Let us consider nuclei undergoing a chemical exchange between 2 equally populated sites A and B with the rate λ (i.e., the lifetime in each site is λ^{-1}). Figure 13a shows the behavior of the magnetizations $\vec{M}_A$ and $\vec{M}_B$ (corresponding to Larmor frequencies $\omega_A<\omega_B$) during the DEFT-sequence in the rotating frame, the frequency of which was set to $(\omega_A + \omega_B)/2$ for the sake of simplicity. The final result is, of course, independent of this assumption. In the case of "slow exchange"**[i.e., $\lambda<\delta$ where $(\delta \equiv 1/2(\omega_B - \omega_A))$] during the first waiting period τ (τ chosen shorter than $\pi/2\delta$), the mixing of both spin populations through the chemical exchange process causes a "pulling together" of $\vec{M}_A$ and $\vec{M}_B$ and, consequently, a retardation of their relative precession as compared with the non-exchange situation ($\lambda=0$). This retardation is transformed to a decrease in time for their convergence through the 180° pulse during the second waiting period τ. As a result $\vec{M}_A$ and $\vec{M}_B$ cross each other in the (-y) direction prior to the final 90° pulse, which then is not able to place $\vec{M}_A$ and $\vec{M}_B$ exactly on the z-axis, thus creating two opposite non-zero components:

$$\vec{M}_{B_X} = - \vec{M}_{A_X}$$

The Fourier transformation of an FID acquired in this way should, therefore, consist (after an appropriate 90° phase-shift relative to the normal Fourier-transform spectrum) of two opposite phase absorption lines, whose amplitudes are simply related to the exchange rate.

---

*If τ is shorter than all T_1's involved.

**We use here the expressions "fast" and "slow" exchange for $\lambda > \delta$ and $\lambda < \delta$ respectively, and not for $\lambda > \delta/2$ and $\lambda < \delta/2$, as it is usually defined in lineshape studies.

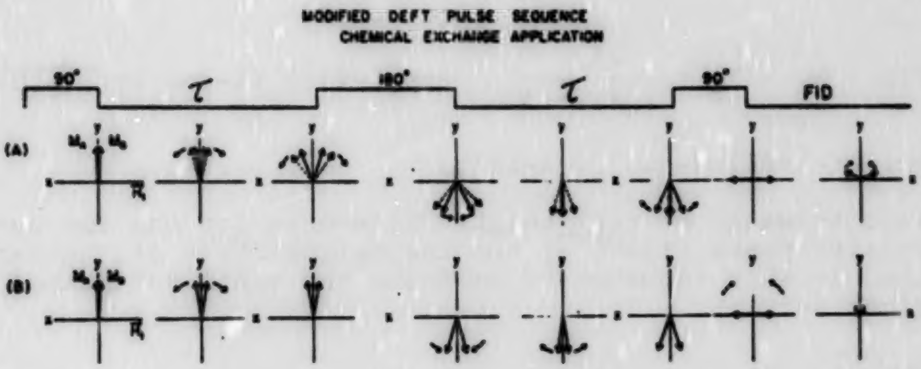
MODIFIED DEFT PULSE SEQUENCE
CHEMICAL EXCHANGE APPLICATION
90°
τ
180°
τ
90°
FID
(A)
(B)
y
x
M_A
M_B
H_1

FIGURE 13. Behavior in the rotating frame of macroscopic nuclear magnetizations in a chemically exchanging 2 site system during the modified DEFT pulse sequence. M_A and M_B and projections in the xy-plane of magnetizations corresponding to the respective spin-populations of both sites A and B; $\vec{H}_1$ is the applied rf field; the polarizing field $\vec{H}_0$ has the direction z. The circular frequency of the rotating frams is arbitrarily set to $\frac{\omega_A + \omega_B}{2}$. (Shortening of $\vec{M}_A$ and $\vec{M}_B$ due to the spin-spin relaxation time is neglected); (a) Slow exchange $(\lambda<\delta)$, τ is chosen smaller than δ^{-1}. Dashed arrows represent $\vec{M}_A$ and $\vec{M}_B$ in the non-exchanging case $(\lambda=0)$, (b) Fast exchange $(\lambda>\delta)$, τ is chosen greater than λ^{-1}.

The modified Bloch-equations (11) for the transverse magnetic components $\vec{M}_A^{tr}$ and $\vec{M}_B^{tr}$ (which are, as usual, represented by complex numbers M_A, M_B) predict the expression (12) for the decay recorded after a DEFT sequence.

$$\frac{dM_A}{dt} = (i\delta-\lambda)\ M_A + \lambda\ M_B$$

$$\frac{dM_B}{dt} = (-i\delta+\lambda)\ M_B + \lambda\ M_A \tag{11}$$

$$\mathrm{FID} = M_A + M_B = \frac{\delta^2\lambda}{(\delta^2-\lambda^2)^{1/2}} \quad \exp\ [-2\lambda\tau]\ (1-\cos\ 2\tau\sqrt{\delta^2-\lambda^2})$$

$$\exp\ [(-\lambda+i\delta)t]-\exp\ [(-\lambda-i\delta)t] \tag{12}$$

The ratio between the peak height difference for the two resulting opposite peaks ($\equiv 2S^{DEFT}$) and the height S^{ECHO} of the Hahn echo (obtained in this sequence by omitting the final 90° pulse) is then given by:

$$\frac{2S^{DEFT}}{S^{ECHO}} = \frac{2\lambda}{\delta}\ (1-\cos\ 2\delta\tau) \tag{13}$$

if second order terms $\propto(\tau^2/\delta^2)$ are neglected. For λ/δ close to 1, the relation between $2S^{DEFT}$ and λ is no longer simple as in (12).

In the case of a "fast exchange" ($\lambda>\delta$), the movement of $\vec{M}_A$ and $\vec{M}_B$ during the DEFT-sequence is shown in Figure 13b. The free precession during the first τ-period has the same Larmor frequency $\frac{\omega_A + \omega_B}{2}$ for $\vec{M}_A$ and $\vec{M}_B$, the two being split apart with and angle (δ/λ), which represents a compromise between their divergent (difference between ω_A and ω_B) and convergent (exchange process) tendencies. Such a configuration is established from an arbitrary initial situation within a time $\sim\lambda^{-1}$, especially after the 180° pulse (which reverses the order of $\vec{M}_A$ and $\vec{M}_B$, so that they have to cross each other afterwards) and after the final 90° pulse (which leaves $\vec{M}_A = \vec{M}_B$), so that the total magnetization has to build up afterwards, starting from zero. The actual FID, recorded after DEFT for the "fast exchange" case is given by (14):

$$\mathrm{FID} = M_A(t) + M_B(t) = \frac{\delta^2\lambda}{2(\lambda^2-\delta^2)^{1/2}} \quad \exp[2\tau(\sqrt{\lambda^2-\delta^2}-\lambda)] +$$

$$\exp\ [-2\tau(\sqrt{\lambda^2-\delta^2}+\lambda)] - 2\ \exp\ [-2\lambda\tau] \quad \cdot \quad \exp\ [(\sqrt{\lambda^2-\delta^2}-\lambda)t] -$$

$$\exp\ (-(\sqrt{\lambda^2-\delta^2}+\lambda)t] \tag{14}$$

It consists of a "slow" and a "fast" exponential term which have opposite signs and cancel each other for t=0. The Fourier transform (phased as in the normal FT experiment) will then be a sum of a narrow positive and a broad negative line. The broad component disappears quickly as (δ^2/τ^2) with rising temperature. The ratio between the height of the positive signal, S^{DEFT}, and the height S^{ECHO} of the Hahn echo is given by (15):

$$\frac{S^{DEFT}}{S^{ECHO}} = \frac{\delta^2}{4\lambda^2} \exp\left[2\tau(\lambda^2-\delta^2-\lambda)\right] + \exp\left[-2\tau(\lambda^2-\delta^2+\lambda)\right] - 2\exp\left[-2\lambda\tau\right] \qquad (15)$$

if only the leading second order-term $(\sim\delta^2/\lambda^2)$ is retained. From the λ^2 denominator in (15), it is clear that S^{DEFT} decreases in slow exchange. On the other hand, the information provided is of more value since λ and δ can in principle be determined from (15) for any given temperature, although the lineshape gives merely their combination, (δ^2/τ).

For the DNMR experiment, in order to achieve the necessary rf homogeneity, a sample of a small volume (as compared to the volume of the receiver coil) had to be used (15mm tube, height of the sample, 23mm) and the spinning of the sample had to be excluded. This still allowed operation at sufficiently high resolution. As a test system for the new technique, we chose the internal hindered rotation in N,N-dimethylacetamide, which we used as a neat liquid (reagent grade, not purified further).

Figure 14a demonstrates the ability of the DEFT sequence to null the transverse magnetization of the acetyl methyl carbon, which is not influenced by the process of internal rotation. The residual signal is on level of ~1% of that observed in a normal FT spectrum. This quality of signal suppression could, however, be reached only over a very narrow spectral window (~100 Hz) close to the carrier frequency (due to finite power and non-rectangular shape of the applied pulses; a width of 100 μsec was needed for a 180° pulse). The investigated N-methyl resonances were then placed in the middle of this range. For each temperature, DEFT and Hahn echo spectra were recorded under identical conditions.

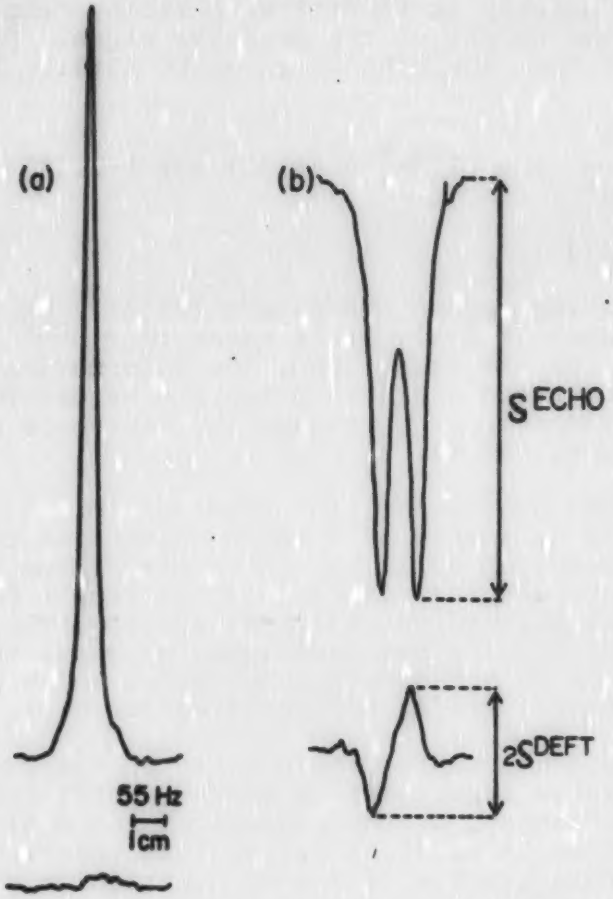

FIGURE 14. (a) The suppression of the acetyl carbon resonance of N,N-dimethylacetamide in the modified DEFT-sequence. On the top is the normal FT spectrum, on the bottom is the spectrum recorded by the modified DEFT-sequence with $\tau=4$ msec. Temperature 73°C (5 Hz artificial line-broadening applied). (b) Resonances of N-methyl carbons recorded as a Hahn-echo, i.e., with the sequence $90°-\tau-180°-\tau$-FID (top) and with the modified DEFT-sequence, i.e., $90°-\tau-180°-\tau-90°$-FID (bottom). The bottom-spectrum is 90° out of phase, $\tau=4$ msec in both cases, Temperature 69.5°C (5 Hz artificial line-broadening applied).

Figure 15 shows the temperature dependence of the signal shape resulting from the application of the DEFT-sequence, which confirms the qualitative theoretical predictions. Table 5 summarizes the results for temperatures far enough removed from coalescense, so that the simple relations (13) and (15) hold. A crude estimate of activation energy from the obtained rates yields $E_a = 18.8 \pm 0.5$ kcal mol^{-1}, in agreement with the value of 19.0 ± 0.1 kcal mol^{-1}, found from lineshape-analysis of the ^{1}H spectra.[23] We feel that optimization of our instrumental facilities should precede a systematic quantitative study and thus we limited ourselves in this case to a demonstration of the feasibility of this kind of analysis.

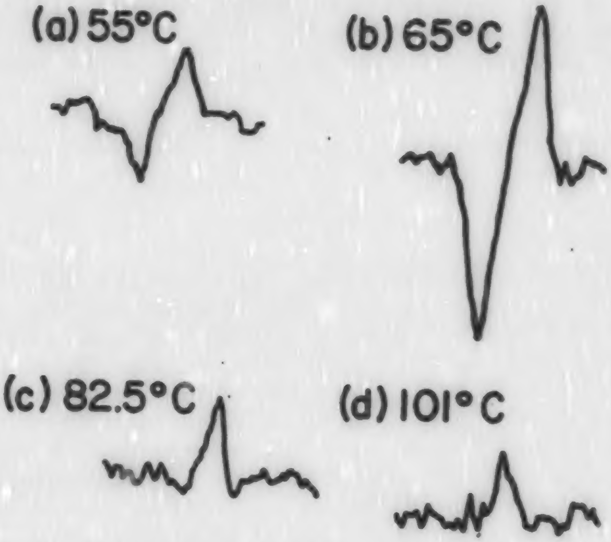

FIGURE 15. The temperature dependence of N-methyl carbons in N,N-dimethylacetamide recorded with the modified DEFT sequence. (a) 55°C, (b) 65°C, (c) 82.5°C, (d) 101°C. (a) and (b) are 90° out of phase. $\tau = 4$ msec. (5 Hz artificial line broadening applied).

---

(23) T. Drakenberg, K. I. Dahlqvist, and S. Forsen, *J. Phys. Chem.*, **76**, 2178 (1972).

TABLE 5. EXCHANGE RATES OF INTERNAL HINDERED ROTATION IN N,N-DIMETHYLACETAMIDE FOR DIFFERENT TEMPERATURES[a]

Temperature (°C)[b]	$\frac{2S^{DEFT}}{S^{ECHO}}$	$\frac{S^{DEFT}}{S^{ECHO}}$[c]	λ^{-1}(msec)
55	0.108		85.6
65.5	0.247		34.7
69.5	0.293		28.5
73	0.415		18.7
101		0.061	2.4

(a) Measured with the modified DEFT pulse sequence. All measurements are made on the N-methyl carbon resonances; (b) Temperatures ±1°C; (c) "fast exchange region".

Summary

The basic requirements for DNMR application of this technique are good rf homogeneity, accurate pulse timing and good pulse shape. This makes its use on current commercial instruments (where these conditions are generally far from being met) highly difficult. We suggest here, nevertheless, some prospective applications in areas where modified DEFT advantages can compensate for experimental difficulties encountered with other known methods. One of these particular features is the facilitated identification of resonances undergoing exchange, as opposed to those that aren't. This can be helpful for analysis of complex spectra. Slowly exchanging resonances can be assigned to each other from their symmetrical periodic dependence on τ (equation 13). The chemical shift differences 2δ can then be determined from (13), even if only one line is resolved. From (13) or (15), δ and λ can be determined independently for each temperature and therefore, no assumptions have to be made about the temperature dependence of these parameters, as in lineshape analysis. Also loosened are requirements of temperature stability of $(T_2^*)^{-1}$, purity of the sample, etc. All of these may be useful in situations where for example, the dependence $\lambda(T)$ is of a complex nature and cannot be described with a single ΔE_a or when the range of temperature variation is limited, as in many biological systems. (In this last case, it is often hard to tell from analysis of the lineshape whether a rate process is actually taking place!) Further, it should be pointed out, that the sensitivity of the method does not become reduced in many cases where other methods become insensitive because exchange makes a comparatively small contribution to the relevant total rate of magnetization decay (i.e., to $(T_2^*)^{-1}$ for lineshape analysis, to $(T_1)^{-1}$ for saturation transfer,[24] to $(T_2)^{-1}$ for echo-train measurements with variable pulse separation[25] and to $(T_{1\rho})^{-1}$ for experiments in the rotating frame). For ^{1}H studies we anticipate that the modified DEFT DNMR methods will not be affected by the presence of homonuclear couplings (provided that the coupling constants are smaller than the chemical shift difference).* The presence of unresolved homo-nuclear couplings presented a serious complication in the lineshape for ^{1}H studies of hindered internal rotation in dimethylformamide (DMF).[26]

---

*This holds for both intramolecular and intermolecular exchange.

(24) S. Forsen and R. A. Hoffman, *J. Chem. Phys.*, **39**, 2892 (1963).

(25) A. Allerhand, and H. S. Gutowsky, *J. Chem. Phys.*, **41**, 2115(1964).

(26) C. Deverell, R. E. Morgan, R. E. and J. H. Strange, *Mol. Phys.*, **18**, 553 (1970).

B. INTERMOLECULAR INTERACTIONS

B1. Chlorophenol Effects on Model Membranes: ESR Study (Collaboration by I. C. P. Smith, et. al.)

The basic work from which arose the idea for a study of the effect of a series of chlorinated phenols on model membrane systems was that of Verma et.al.(27) In that paper Verma reported observing, for certain uncouplers of oxidative phosphorylation, a disordering effect on the degree of order or organization of phospholipids in hydrated multibilayers. Verma monitored these effects on the phospholipids by using the cholestane spin probe (CSL) incorporated into the multibilayers. One of the uncouplers studied was pentachlorophenol (PCP). He found that at PCP concentrations of $2\text{x}10^{-5}$M in hydrating buffer, the multibilayers of egg lecithin-cholesterol (2:1 mole ratio) were maximally disordered at the pH corresponding to the pK of the PCP. This disordering effect was intensified when the multibilayers were composed only of egg lecithin, and it was maximal at a pH different from that of PCP's pK. The series of experiments suffered from a reliance on having to note and interpret a very small change in the CSL's EPR spectrum. This special parameter is not only sensitive to the effects of the PCP on multibilayer, but also depends on the experimenter's ability to make the films (it is difficult to obtain near identical films). Despite these problems, Verma felt he was observing a real disordering effect of PCP on multibilayers.

Given this then, a series of chlorinated phenols were proposed for a new study using the spin label ESR technique just as in Verma's study. To date the experiments have largely been of a preliminary nature involving only three compounds of the series: phenol, 2,3,5-trichlorophenol and 2,3,5,6-tetrachlorophenol. Two model systems have been used to prepare the multibilayers; egg lecithin-cholesterol (2:1 mole ratio), and decholesterolized brain lipid. The spin probe has been CSL in all cases, and the buffer (pH 2 to 12). The three phenol-like compounds have been made up at each pH to $4\text{x}10^{-5}$M and thus all reported observations and effects are due to the perturbing effects of the compounds at this physiologically reasonable concentration.

The effects of these compounds on the multibilayers have not been pronounced as Verma interpreted PCP to exert. When egg lecithin-cholesterol multibilayers were hydrated with $4\text{x}10^{-5}$M phenol at integral pH values between 2 and 12, no disordering effect was observed in the spectra. Even when the hydrating buffers contained $2\text{x}10^{-5}$M phenol, the disordering effect, if the data can truly be interpreted as such, would be very small (less than 10% in terms of the parameter measured, which may not be above experimental error). While it appears that no disordering effect is made manifest by the phenol, these experiments should be repeated since they were performed while in the process of learning good film making technique, and also because no re-equilibration experiments were attempted with these films.

---

(27) S. P. Verma, H. Schneider and I. C. P. Smith, *Archives Biochem. and Biophys.*, **154**, 400 (1973).

The most extensively studied system has been the egg lecithin-cholesterol multibilayers; first hydrated with buffered $4\times10^{-5}\underline{M}$ 2,3,5,6-tetrachlorophenol, and then re-equilibrated with the appropriate pH buffer. The results here have been contradictory: one time indicating increased order after re-equilibration with buffer (i.e., a disordering effect by the chlorophenol with an effect maximal near the pK of the compound), and the other time a very small disordering effect being observed equally at all pH's. When the films were hydrated in the reverse order (with buffer and then re-equilibrated with buffer plus the chlorophenol), the effect was essentially zero since some pH's showed small negative changes while others showed small positive ones.

In like manner,when egg lecithin-cholesterol films were hydrated first with $4\times10^{-5}\underline{M}$ 2,3,5-trichlorophenol buffers and then re-equilibrated with buffers, a small disordering effect for the chlorophenol was noted over all pH's. This disordering effect of the trichlorophenol needs to be validified with more experiments just as in the case of the tetrachlorophenol compound.

Only one system seems to have given definite positive proof for the disordering effect of 2,3,5,6-tetrachlorophenol at $4\times10^{-5}\underline{M}$, pH 6.00. This system is multibilayer films composed of de-cholesterolized brain lipid containing an added 8 gm% cholesterol. With this cholesterol content the brain lipid has just passed through its gel-liquid crystal phase transition, and is in the liquid crystal phase. Since it is right at the transition point, the system is very responsive to disordering effects back to the gel. This is in fact what one observes by monitoring films labelled with CSL and hydrated with the chlorophenol. When the multibilayers are hydrated with buffer first and a spectrum recorded, and then re-equilibrated with buffer containing $4\times10^{-5}\underline{M}$ 2,3,5,6-tetrachlorophenol for 3-7 days, interpretable spectral differences are obtained. Using the method of Neal et.al.* one obtains molecular order parameters for the CSL in the two hydration cases. After a 3 day re-equilibration with the tetrachlorophenol buffer, the order parameter decreased 23% from the original order parameter obtained after buffer hydration. After 7 days, the order parameter for the same film was 28% less than the starting value. While the careful control film and pH correction were lacking in arriving at these decreases in the order parameter, the disordering effect of the tetrachlorophenol is still regarded as real.

---

*Pre-publication procedure, expected to be published in Molecular Pharmacology.

These results have implications for future experiments which may lead to improved quality results. Certainly the time scale in which chlorophenols are allowed to exert their effects should be increased. Secondly, the low cholesterol brain lipid system may be a better system than the egg-lecithin cholesterol one for observing the effect of the compounds. In progress also are some experiments using multilamellar dispersions. These should be valuable in manifesting chlorophenol effects since the two dispersions tried to date have given some promising results which may be interpretable with some amended experimental procedures.

B2. Chlorophenol Effects on Model Membranes: ^{13}C NMR Study

Simultaneously with the new ESR work on chlorophenol incorporation into model membranes, a supportive ^{13}C nmr study was begun.

There are two main disadvantages to the nmr techniques; (1) The membrane models are imperfect (vesicle bilayers); (2) A high concentration of "membrane" component is required.

Offsetting these disadvantages is the fact that ^{13}C nmr methods are capable of giving us a more detailed look at the actual process of disruption of the membrane model system.

Using ^{13}C spin-lattice relaxation times (T_1's) we are able to evaluate the form of the effect of the chlorinated phenols on the model membranes. The potential information obtainable from the nmr data is more detailed than that available from the ESR experiments. However, it should be pointed out that the overall order parameter (ESR data) is generally more sensitive to membrane structure than is the mobility of the lipid alkyl chains (as measured by ^{13}C T_1's).

Preliminary 67.9 [illegible] ^{13}C T_1 data on 5 sonicated dispersions of synthetic d,ℓ-dipalmitoyl lecithin (DPL) are shown in Table 6. In these experiments we are able to observe the internal and overall mobility of the lecithin bilayers with added 3,5-dichlorophenol (DCP), 2,3,5,6-tetrachlorophenol (TCP), pentachlorophenol (PCP) (2 concentrations), and without incorporation of any foreign compounds.

The data in Table 6 are preliminary. However, they already indicate one important and somewhat unexpected result of pentachlorophenol incorporation into the bilayer structure.

^{13}C relaxation data (T_1's and/or T_2's) for individual carbons in DPL bilayers indicate the general degree of mobility of the long alkyl chains in the hydrophobic portion (of the bilayers). They also give insight into the overall motional freedom of the DPL molecules, using the relatively anchored group resonance C-2 as the monitor.

TABLE 6. ^{13}C RELAXATION DATA IN MODEL MEMBRANE SYSTEMS INCORPORATING CHLORINATED PHENOLS

	^{13}C T_1(sec)[b]					
SOLUTION[a]	C-2	C-3	C-4 to C-13	C-14	C-15	C-16
DPL	.55	.75	~0.95	2.2	3.8	6.6
DPL, 0.01M PCP	.46	.55	~0.72	2.7	2.5	5.9
DPL, 0.04M DCP	.44	.55	~0.82	1.7	2.8	5.0
DPL, 0.04M PCP	1.5	1.6	~1.0	2.3	2.9	5.6
DPL, 0.04M TCP	0.8	0.5	~1.0	2.5	2.5	4.6

[a] DPL - synthetic dipalmitoyl lecithin, (0.3M), PCP - pentachlorophenol, DCP - 3,5-dichlorophenol; TCP - 2,3,5,6-tetrachlorophenol; [b] at 63° and 67.9 MHz; Accuracy, ±15% (estimated).

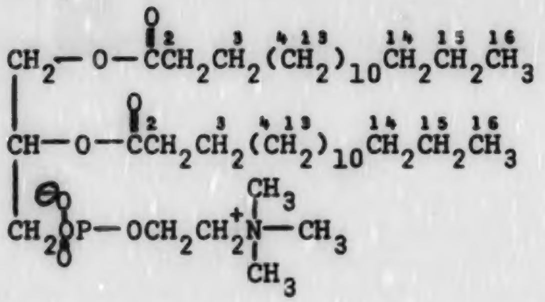

FIGURE 16. Dipalmitoyl Lecithin (Phosphatidyl Choline)

In the micellar DPL solutions containing 0.01M PCP or 0.04DCP, no definitely significant trends were noted. It is possible that the hydrophobic inner portion of the bilayers has somewhat reduced segmental motion. Unfortunately, the present preliminary data are not sufficiently accurate nor reproducible to confirm this possibility.

On the other hand, one surprising fact emerges from these first experiments. The ^{13}C T_1's for C-2 and C-3 in the DPL solution containing 0.04M PCP clearly show a substantial loosening up of the polar end of the alkyl chains. Interestingly, the polar head groups themselves do not show significant increased mobility except at one carbon (see Table 7); just the C-2 and C-3 (plus presumably the unresolved C-4 and C-5) methylene groups undergo increased motion. The lengthening of T_1 by a factor of $\overline{>}3$ (as for C-2 and C-3) corresponds to an increase in motion by a factor of 3 to ~9, depending on which theoretical model is chosen.*

Our first experiment with 2,3,5,6-tetrachlorophenol is inconclusive. However, it appears the TCP may be affecting the bilayer structure significantly.

Table 7 summarizes ^{13}C T_1 data for the same solutions, but in this case listing the polar head groups. As stated above, the glycerol residue mobility does not appear to be affected by PCP incorporation. The preliminary data do indicate that the choline OCH_2 group may be experiencing increased motion with PCP incorporation. This apparent result is being verified currently.

While we might now propose a model showing pentachlorophenol to incorporate within a specific area of the bilayer structure we feel that such a model would be premature.

A much stronger case for any model will undoubtedly arise from intended variable field ^{13}C T_1 measurements on DPL and egg lecithin bilayers, incorporating PCP, TCP, and other materials.

TABLE 7. ^{13}C T_1 DATA FOR THE GLYCEROL AND POLAR HEAD GROUP RESIDUES

	^{13}C T_1(sec)[a]			
SOLUTION	$^{+}NMe_3$	glycer	choline $-OCH_2$	choline $-NCH_2$
DPL	1.24	0.16	0.55	0.73
DPL, 0.01M PCP	1.32	0.13	0.67	0.75
DPL, 0.04M DCP	1.18	0.17	0.66	0.8
DPL, 0.04M PCP	1.25	0.16	0.35	0.83
DPL, 0.04 TCP	1.15	n.m.	n.m.	n.m.

[a] At 67.9 MHz and 63°; Accuracy ± 15-25% (estimated).

---

* See for example: G. C. Levy, J. Am. Chem. Soc., 95, 6117 (1973).

B3. Variable Field NMR Experiments on Model Membranes.

As a result of research finished or underway in our laboratory (see sections B4 and E) we can now project significant new information to be derived from multi-field ^{13}C T_1 measurements on DPL and other model membrane bilayers, incorporating chlorophenols and other materials.

This summary forms an initial informal disclosure of this anticipated expansion of scope.

It has been noted above that both ESR spin-labeling measurements[27] and ^2H nmr measurements[28] can be useful for characterization of the order parameter in bilayer structures. ^{13}C T_1 measurements on the other hand have not elucidated higher order in membrane models. The main advantage of ^{13}C nmr measurements has been their ability to probe the various structural parts of the molecular system. This is in contrast to the overall nature of the spin-labeling experiments. Deuterium nmr experiments using specific isotope labeling can give increased information. However, those experiments require large experimental efforts and may be impractical for extended pesticide incorporation studies. In the limited ^2H work reported, the order parameters were appreciably lower than as obtained from ESR spin-label measurements. This ambiguity is thought to result from spin-label perturbations or from differences of nmr and esr method sensitivities to short-lived deformations of the bilayer structure.[28]

The variable field ^{13}C T_1 measurements beginning now may prove to be a sensitive new probe into membrane structure since they probe molecular motion at each carbon site and also since the cooperativity of the chain motions will be probed. Thus, a parameter bridging and complementing previously available data will be developed. Previous ^{13}C T_1 studies of model membranes have been conducted at one magnetic field, and thus this extra information was not obtainable. Computer programs are under development in this laboratory to interpret the variable field data in terms of physically realistic models.

---

(28) H. H. Mantsch, H. Saito and I. C. P. Smith, in a review in Prog. in NMR Spectrosc., J. W. Emsley, J. Feeney and L. H. Sutcliffe, eds., (Pergamon Press), in press.

B4. Variable Field ^{13}C T_1 Studies of complex Systems

Two projects near completion in our laboratory are examining the effect of magnetic field on ^{13}C T_1 measurements. In one project (see Section E) we are extending previous models of complex chain molecular motions in polymers. In the second project we are probing cooperative long time-scale motional components for the carbons of relatively small associated molecules, such as alcohols, glycols, carboxylic acids, etc.

In these cases we are confirming anticipated magnetic field dependencies for carbons undergoing insufficient motion to be in the "extreme narrowing" limit. But, more importantly, we are learning that in many cases cooperative long time-scale motional components may strongly influence molecular dynamics for carbon groups apparently reorienting rapidly enough to be well within the nmr motional narrowing limit (to $\lesssim 10^{-12}$ sec!).

In 1,2-decanediol the strongly associated glycol function results in a large degree of observed segmental motion. This is clearly seen in the increasing T_1 values for carbons successively removed from the hydroxyl groups. This observation of segmental motion is not unexpected, since the situation is quite close to that observed for 1-decanol in 1971 by Doddrell and Allerhand.[29]

New information may be derived from the fact that all 10 carbons of 1,2-decanediol exhibit a significant dependence on magnetic field, despite the fact that according to its observed T_1 even the motionally restricted C-2 CH carbon does not significantly violate the condition of "extreme spectral narrowing".[30,31] At 67.9 MHz, dipolar T_1's (CH) of less than ~400 msec (corresponding to $\tau_c \gtrsim 10^{-10}$ sec) increasingly deviate from T_1's obtained at lower field. The large dependence of these T_1's on the experimental Larmor frequency can be explained if the molecular dynamics is not explainable in terms of one, two, or three discrete effective correlation times. Instead it is necessary to invoke a distribution of correlation times, with some motional components that are relative slow. The interesting point here, is observation of a large field dependence not only for the C-1 and C-2 carbons, but for all of the carbons of the pendant carbon alkyl chain.

---

(29) D. Doddrell and A. Allerhand, J. Am. Chem. Soc., 93, 1558(1971).

(30) A. Abragam, "The Principles of Nuclear Magnetism," Oxford Press (Oxford) 1961, p. 299 ff.

(31) J. R. Lyerla and G. C. Levy, in Topics in Carbon-13 NMR Spectroscopy, 1, 88 (1974).

TABLE 8. ^{13}C SPIN-LATTICE RELAXATION TIMES FOR 1,2-DECANEDIOL AND SEVERAL SIMILAR MOLECULES.

			^{13}C T_1(sec)^c									
Compound[a]	Temp(°C)[b]	Frequency MHz	C-1	C-2	C-3	C-4	C-5	C-6	C-7	C-8	C-9	C-10
1,2-decane-diol	54	22.6	0.26	0.41	0.30	0.36	---	∿0.5	---	0.95	1.5	3.4
	54	67.9	0.5	0.80	0.60	0.75	---	∿0.9	---	1.8	2.7	5.3
1-decanol[d]	37	22.6	0.7	0.7	0.7	---	---	∿1.0	---	1.5	2.4	3.9
	37	67.9	0.6	0.6	0.7	---	---	∿1.0	---	1.4	2.3	3.8
n-eicosane	49	22.6	6.0	4.0	2.8			1.4				
	49	67.9	5.9	4.3	3			1.4				

[a] Samples neat;

[b] Temperature ±2°, measured directly before and after data collection;

[c] Maximum probably error ±5-15%. Decanediol data, average of two runs: reproducibility was ±3% except for C-3 and C-10 (at 22.6 MHz);

[d] Preliminary data, ±10-15%.

Metcalfe, Levine, and co-workers have developed a theory which predicts that 5 $CH_2 - CH_2$ bonds are sufficient to decouple the motion of a straight chain CH_2 group from a site of restriction.[32,33] The two field $^{13}CT_1$ data for the "pendant" eight carbon chain of 1,2-decanediol indicate that the published theory is not valid at least for this molecular system.

We are currently investigating theoretical models for chain segmental motion, using two field ^{13}C relaxation data from solutions of poly-(*n*-butyl) and poly-(*n*-hexyl) methacrylates. The polymer main and side chain T_1's cover a wide range of values, some apparently within the region of extreme spectral narrowing. A significant field dependence was noted for all carbon T_1's and in addition, a complex behavior was observed for the ^{13}C [^{1}H] NOE's. While this theoretical work is not yet completed, it does indicate that when long time-scale motions are mixed with faster motional components (resulting in a distribution), T_1's will be strongly frequency dependent over a wide range of effective correlation times (τ) including the region of extreme spectral narrowing.

(32) Y. K. Levine, N. J. M. Birdsall, A. G. Lee, J. C. Metcalfe, P. Partington and G.C.K. Roberts, J. Chem. Phys., 60, 2890 (1974).

(33) Y. K. Levine, P. Partington, and G. C. K. Roberts, Mol. Phys., 25, 497 (1973).

Our calculations show that even a small contribution from long time-scale motions will affect T_1's significantly, but will affect NOE's considerably less (see section E for details).

Thus, all of the T_1 field dependences for 1,2-decanediol can be explained with a model of cooperative segmental motions superimposed on a slow overall molecular reorientation. The slower motions are incompletely decoupled from the segmental motions of the chain carbons, including the C-10 CH_3 group.

In order to validate the unexpected experimental results obtained here, variable field T_1's were obtained on the alkane n-eicosane (Table 8). No field dependence was noted for this non-associated molecule.

In another experiment 1-decanol was examined (see Table 8). The preliminary data do not show an unequivocal field dependence for this alcohol. If the final numbers show an insignificant field dependence, then this will indicate that segmental motion, as observed in this simple alcohol, is not strongly cooperative as in the diol. Further experiments are underway to investigate the effects of structure, solvent, and temperature on cooperativity of molecular motion.

C. INTERACTIONS OF CHLORINATED PHENOLS: HYDROGEN BONDING

As an initial step to the understanding of chlorophenol intermolecular interactions, we undertook a study of self association of three dichlorophenols and model compounds. That study gave us insight into the differences resulting from ortho versus meta or para halogen substitution. The initial disclosure of our results has been published in the Journal of Physical Chemistry 79(21):2325-2326, 1975. [A more complete manuscript is in preparation; it should be ready for submission for publication in fall 1977].

D. ANALYSIS OF POLYCHLORINATED BIPHENYLS BY CARBON-13 NUCLEAR MAGNETIC RESONANCE SPECTROSCOPY.

Aroclors, which are mixtures of polychlorinated biphenyls, have been used extensively as insecticide synergists[34] in the United States (a synergist is a compound which enhances the relativity of another compound to which it is added). Although the use of Aroclors in the United States is currently highly restricted, they are still being used in large quantities in other countries. In spite of the current restrictions on their use in the United States, Aroclors continue to enter our environment today. These materials have high toxicity.[35] It is desirable to develop a quick method for the analysis of these complex mixtures.

In recent years, the use of carbon-13 nuclear magnetic resonance has become significant for identification of organic compounds and also for quantitative analysis of simple mixtures.[36] The recent growth of applications for ^{13}C nmr followed major instrumental advances in the early 1970's. The advantages of ^{13}C spectroscopic techniques include ultrahigh resolving power with a chemical shift range of over 200 ppm, compared with ~10 ppm for proton chemical shifts. ^{13}C spectrometers operating at high magnetic fields have particularly high resolving power, especially when utilizing broadband proton decoupling techniques that make it possible for ^{13}C resonances to be (generally) observed as sharp singlets. One major drawback for ^{13}C nmr methods of chemical analysis is the relatively low sensitivity (in the sense of required sample size) for this technique, when compared with optical spectroscopies, and ^{13}C nmr is far less sensitive than ^{1}H nmr. Nevertheless, the increased information available from nmr spectroscopies and ^{13}C spectra in particular, allows these techniques to be advantageous in some instances.

Problems are known to exist in "quantitative" ^{13}C analysis. A major problem arises from the need for relatively long delays between time-averaged acquisitions of spectra. These relatively long delays (sometimes > 1 min.) are caused by the need to allow complete relaxation of each nuclear spin (^{13}C nucleus) between data acquisitions. It is necessary to wait at least 3-4 times the

---

(34) O. T. Sanders, R. L. Zepp, and R. L. Kirkpatrick, *Bull Environ. Contam. Toxicol*. **12**, 394 (1974); (b) N. S. Fisher, E. J. Carpenter, R. C. Remsen, and C. F. Wurster, *Microb. Ecol*., **1**, 39 (1974); (c) S. Innami, H. Tojo, Y. Utsuyi, A. Nakamuia, and S. Naguyama, *Eiyogaku Zasehi*, **32**, 58 (1974).

(35) H. Berge, *Naturwiss Rundsch*, **27**, 447 (1974).

(36) G. C. Levy and G. L. Nelson, "Carbon-13 Nuclear Magnetic Resonance for Organic Chemists," 1972; J. B. Stothers, "Carbon-13 NMR Spectroscopy," 1972; E. Breitmaier, "^{13}C NMR Spectroscopy," 1974.

spin-lattice relaxation time (T_1)[37] to allow this complete relaxation. This waiting period can be circumvented using commercially available paramagnetic relaxation reagents such as (Tris) acetylacetonatochromium III ($Cr(acac)_3$) which shortens spin-lattice relaxation times for carbons not having efficient relaxation pathways.[38] Once the spin-lattice relaxation time has been decreased to $\lesssim$0.3 sec, it is then possible to greatly expedite data acquisition. Use of these relaxation reagents also helps to overcome another problem. As a result of the complete proton decoupling used to obtain singlet resonances in ^{13}C spectra, there is normally a perturbation of spectral peak intensities attributable to the nuclear Overhauser effect. NOE's may affect different carbons to a varying extent thus peak intensities may be misleading. The relaxation reagents, under proper conditions,[38] can effectively suppress the nuclear Overhauser effect for all carbons.

The spin-lattice relaxation times for several individual polychlorinated biphenyls have been reported previously by Wilson.[39] These T_1's were observed to be 2-5 seconds for C-H carbons. The carbons not having directly bonded hydrogens have T_1's which were considerably longer, as expected. $Cr(acac)_3$ added at a concentration near 3×10^{-2}M decreases these T_1's to under 0.5 seconds. Thus the time required for the experiment is decreased, and NOE's can be effectively suppressed for all non-proton bearing carbons (C-Cl and C-1 carbons).

A major method for study of Aroclors is gas-liquid chromatography (g.l.c.). This method, although accurate, can be time consuming since samples are often of insufficient purity for direct g.l.c. analysis. Although direct ^{13}C nmr analysis is not as versatile for analysis of chlorinated biphenyl mixtures, in some cases it can provide useful information very rapidly. Unlike g.l.c., ^{13}C spectra on large samples can be obtained in seconds or minutes and sample preparation may only require dissolution in a solvent. Many materials which might prove disastrous to g.l.c. experiments can be easily handled. One major advantage, of course, for g.l.c. is the very small amount of sample required for analysis. In all Aroclor systems examined in this study, sufficient samples were available. Figure 17 shows the spectrum of Aroclor 1221 obtained without the use of $Cr(acac)_3$; Figure 18 shows the result with added relaxation reagent.

(37) J. R. Lyerla and G. C. Levy, "Topics in Carbon-13 NMR Spectroscopy," Vol. 1, G. C. Levy, Editor, 1974, Chapter 3.

(38) G. C. Levy and Ulf Edlund, J. Am. Chem. Soc., **97**, 4482 (1975) and references cited within.

(39) N. K. Wilson, J. Am. Chem. Soc., **97**, 3573 (1975).

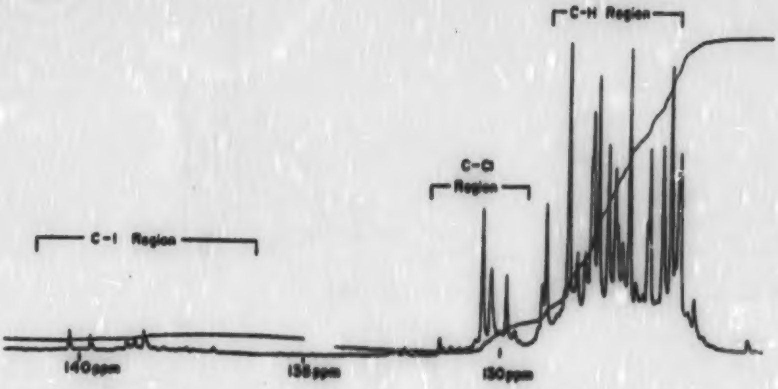

FIGURE 17. 67.9 MHz ^{13}C NMR Spectrum of Aroclor 1221 (Aromatic region shown). No paramagnetic relaxation reagent added; 300 scans, 8 sec scan interval.

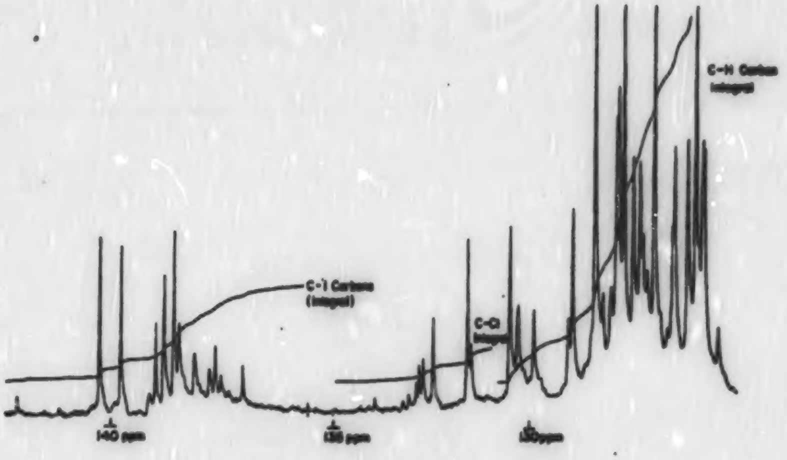

FIGURE 18. 67.9 MHz ^{13}C NMR Spectrum of Aroclor 1221 (Aromatic region shown). 3×10^{-2} $\underline{M}$ relaxation reagent ($Cr(acac)_3$) added; 300 scans, 1 sec scan interval.

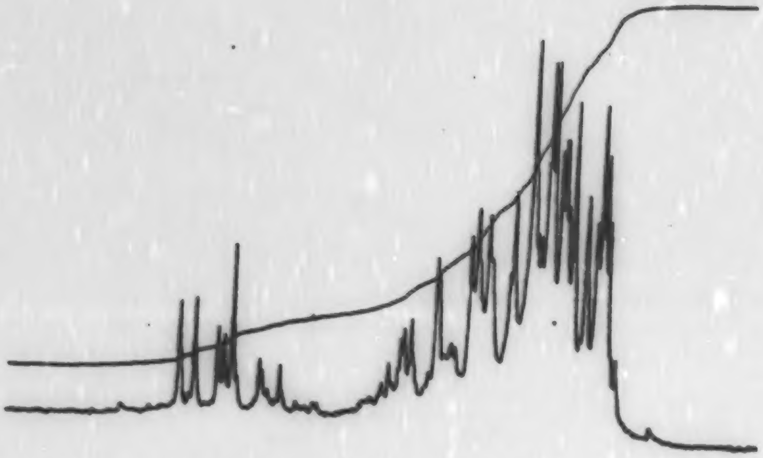

FIGURE 19. 67.9 MHz ^{13}C NMR Spectrum of Aroclor 1232, chlorine content 32%. 3 x 10^{-2}M relaxation reagent added. 300 scans, 1 sec scan interval.

TABLE 9. COMPOSITION AROCLOR 1221

Chlorine Substitution	Mole %	G.C. 40
Nil	≤ 10%	+
2	≈ 17%	+
3	< 3%	+
4	≈ 17%	+
2, 2'	≤ 11%	+
3, 3'	< 3%	+
4, 4'	≈ 5%	+
2, 6	undetectable	-
3, 4	20%[a]	+
2, 4, 2', 4'	undetectable	-
2, 5, 2', 5'	< 3%	-
2, 6, 2', 6'	undetectable	-
3, 4, 3', 4'	undetectable	-
3, 5, 3', 5'	< 3%	-
2, 3, 5, 6	undetectable	-

The spectra in Figures 17 and 18 illustrate the dramatic changes upon the addition of Cr(acac)$_3$. The carbons normally having long T_1's and lower NOE's (C-Cl and C-1 carbons) are more easily observed with the relaxation reagent. ^{13}C chemical shifts for each of the individual isomers composing an Aroclor mixture had been previously determined by Wilson,[39] and with this information available, assignments for the Aroclors were greatly facilitated. The high magnetic field employed (63 kGauss) to obtain the spectra enhanced peak identification by increasing the resolution over normal (14-23 kGauss) field ^{13}C NMR spectrometers. To make assignments of peaks more straightforward, isomers containing more than four chlorines were not considered (the mixture is known to contain on an average 1.2 chlorines/molecules). The relative intensities of the assigned peaks were then assumed to be proportional to the particular isomer concentration in the mixtures. For the above procedure to be valid the relaxation time with Cr(acac)$_3$ present must be short ($\lesssim$0.5 sec) and also the NOE's must be equivalently suppressed. The ^{13}C T_1's for all carbons in a representative Aroclor were measured in the presence of 3×10^{-2}M Cr(acac)$_2$; the measured value was 0.4 seconds. This is sufficiently short to fill both requirements.

^{13}C analysis of Aroclor 1221 is given in Table 9. Quite good agreement with g.l.c. analysis[40] can be noted. As one check on the quantitative accuracy, a total chlorine analysis was obtained from the spectra using relative peak intensities. The total chlorine content from this method (1.4 atoms per molecule) does not agree quantitatively with the stated Aroclor chlorine content (1.2 atoms per molecule).[41]

Direct analysis of heavily chlorinated mixtures of PCB's is far more difficult since there are a larger number of compounds present and it is very difficult to assign peaks by manual ~~me~~ methods.[42] Figure 19 shows the partially interpreted spectrum of Aroclor 1232 (32% chlorine). Future computer analysis of similar spectra should extend analysis to at least 50% and possibly higher total chlorine content.

(40) G. Webb and A. C. McCall, J. of A.O.A.C., 55, 746 (1972).

(41) However, the semi-quantitative agreement is gratifying since this type of determination, using both C-Cl and C-H carbon resonances, is not expected to be as accurate as isomer determination which uses resonance lines arising from similar type carbons.

(42) Even the Avoclor 1232 sample analysis proved difficult.

E. CHAIN MOLECULAR DYNAMICS IN COMPLEX MOLECULES

As equipment and relaxation measurement techniques have become more sophisticated and sensitive in the last few years[43], the amount of molecular dynamics information which can be obtained by nmr has increased greatly.[44-47] As these experiments become more accurate, the possibility of elucidation of more subtle molecular dynamic processes is also enhanced. These additional consequences of the development of the field result in other problems, namely, the analysis of any relaxation data presupposes that an adequate model has been chosen. The generally accepted approximation of a single correlation time characterizing the exponential decay of the autocorrelation function has been the preferred choice for most analyses.[48-55]

---

(43) D.I. Hoult, Specialist Periodical Reports, vol. 5 (Chem. Soc.).

(44) R. L. Somorjai and R. Deslauriers, J. Am. Chem. Soc., 21, 6460 (1976).

(45) K. Levine, P. Partington, G. C. K. Roberts, N. J. M. Birdsall, A. G. Lee and J. C. Metcalfe, FEBS Letters, 23, 203 (1972).

(46) K. Levine and N. J. M. Birdsall, A. G. Lee and J. C. Metcalfe, Biochemistry, 11, 1415 (1972).

(47) D. Robinson, N. J. M. Birdsall, A. G. Lee and J. C. Metcalfe, Biochemistry, 11, 2903 (1972).

(48) A. Abragam, "The Principles of Nuclear Magnetism", Oxford University Press, London, Chapter 8.

(49) T. C. Farrar and E. D. Becker, "Pulse and Fourier Transform NMR", Academic Press, New York, 1971.

(50) D. Doddrell, V. Glushko and A. Allerhand, J. Chem. Phys., 56, 3683 (1972).

(51) J. Granjean and P. Laszlo, Mol. Phys., 30, 413 (1975).

(52) A. Allerhand and R. A. Komoroski, J. Am. Chem. Soc., 95, 8228 (1973).

(53) H. Saito, H. H. Mantsch and I. C. P. Smith, J. Am. Chem. Soc., 95, [illegible] (1973).

(54) M. C. Fedarko, J. Magn. Resonance, 12, 30 (1973).

(55) G. C. Levy, Accounts Chem. Resonance, 6, 161 (1973).

Recent theoretical advances[56-65] have allowed for the interpretation of more complex molecular motions, but extensive variable temperature and variable frequency experiments have not been available to properly test each model. Such testing should in theory encompass measurement of all three accessible parameters: the spin-lattice relaxation time, T_1, the spin-spin relaxation time, T_2, and the nuclear Overhauser enhancement, NOE.

We report here the results of an investigation of two polymers, poly(n-butyl methacrylate) and poly(n-hexyl methacrylate) at a number of temperatures and at two widely different magnetic fields. The inadequacies of the available models will be discussed and suggestions for improvement of the present theories will be proposed.

Experimental

Poly(n-butyl methacrylate) (PBMA) was obtained from Polyscience, Inc. as a high molecular weight material. Solutions were made without further purification using toluene-d_8 and benzene-d_6 as solvents. Poly(n-hexyl methacrylate) (PHMA) was purchased as a toluene solution (25wt%) from the Aldrich Chemical Company. All samples were sealed in nmr tubes but not degassed. 50% PHMA samples were prepared by solute concentration at ~70° under a N_2 gas stream.

Natural abundance ^{13}C spectra were obtained using Bruker HX-270 and HFX-90 spectrometers operating for ^{13}C at 67.9 MHz and 22.6 MHz, respectively. Free induction decays were accumulated using Nicolet 1080 series computers and Fourièr transformed to yield 4096 data points in the frequency domain spectra.

---

(56) S. Berger, F. R. Kreissel, D. M. Grant and J. D. Roberts, *J. Am. Chem. Soc.*, **92**, 1805 (1975).

(57) D. E. Woessner and B. S. Snowden, Jr., *Adv. Mol. Relaxation Proc.*, **3**, 181 (1972).

(58) D. E. Woessner, *J. Chem. Phys.*, **36**, 1 (1962).

(59) D. Wallach, *J. Chem. Phys.*, **47**, 5258 (1967).

(60) Y. K. Levine, P. Partington, and G. C. K. Roberts, *Mol. Phys.*, **25**, 497 (1973).

(61) Y. K. Levine, N. J. M. Birdsall, A. G. Lee, J. C. Metcalfe, P. Partington, and G.C.K. Roberts, *J. Chem. Phys.*, **60**, 2890 (1974).

(62) R. E. London and J. Avitabile, *J. Chem. Phys.*, **65**, 2443 (1968).

(63) W. T. Huntress, Jr., *J. Chem. Phys.*, **48**, 3524 (1968).

(64) L. G. Werbelow and D. M. Grant, *J. Chem. Phys.*, **63** 544 (1975).

(65) L. G. Werbelow and D. M. Grant, *J. Chem. Phys.*, **63**, 4742 (1975).

Quadrature detection was employed for all T_1 experiments and some of the NOE determinations.

T_1 measurements were performed using the $(T\text{-}180°\text{-}\tau\text{-}90°)_n$ Fast Inversion Recovery pulse sequence, FIRFT.(66) Intensities obtained from the FIRFT spectra were used to calculate relaxation times using the expression $\ln(S_\infty - S_\tau) = \tau/T_1$ where S_∞ is the equilibrium amplitude of the fully relaxed peak and S_τ is the amplitude of the peak at some pulse delay time τ. The estimated error in T_1 is approximately 10%, but repetitive measurements indicated that the reproducibility was much better.

Nuclear Overhauser enhancements, NOE values, were determined with gated decoupling(67) generally using single phase detection. Experiments were set up to take two sets of spectra: two were acquired with constant wideband decoupling and two others using interrupted decoupling. The pulse interval equalled or exceeded ten times the longest T_1 involved. NOE values were determined from the average of the two data sets and are considered accurate to within ±15%-20%.

The temperature was controlled with a Bruker B-ST100 heating unit. The sample temperature was measured using a thermometer placed in an equivalent sample tube containing an equivalent volume of benzene of toluene solvent, under identical decoupling conditions. Decoupling power was kept low to prevent sample heating during gated decoupling NOE measurements (~3-4 watts).

All theoretical calculations were performed on a CDC 6400 computer with programs written in FORTRAN IV.

Theory

For two nonequivalent spin-1/2 nuclei the spin-lattice relaxation time[48,49] (T_1) and the nuclear Overhauser enhancement factor (NOEF) may be written in terms of the spectral density functions, $J_i(\omega)$, as:

$$\frac{1}{T_1} = 0.1\, N\, \gamma_C^2 \gamma_H^2 \hbar^2 r^{-6} [J_o(\omega_H - \omega_C) + 3J_1(\omega_C) + 6J_2(\omega_H + \omega_C)] \tag{15}$$

and

$$\text{NOEF (NOE-1)} = \eta = 3.976 \left[\frac{6J_2(\omega_H + \omega_C) - J_o(\omega_H - \omega_C)}{J_o(\omega_H - \omega_C) + 3J_1(\omega_C) + 6J_2(\omega_H + \omega_C)} \right] \tag{16}$$

(66) However, these experiments were normal IRFT measurements for all but the longest T_1 carbons.

(67) R. K. Harris and R. H. Newman, Ibid., **24**, 449 (1976).

where N is the number of directly attached hydrogens (for $^{13}C-^{1}H$ dipolar relaxation), γ_C and γ_H are the magnetogyric ratios of carbon and hydrogen respectively, and r is the carbon-hydrogen internuclear distance.

If the autocorrelation function can be described[48] by an exponential characterized by a single correlation time, τ_c:

$$J_i(\omega) = \frac{\tau_c}{1 + \omega^2\tau_c^2} \tag{17}$$

For a distribution of correlation times[68-74] (mathematically indistinguishable from a non-exponential autocorrelation function) one can introduce a multiplicative factor known as the probability destiny function, $G(\tau_c)$,[68] and equation (17) becomes

$$J_i(\omega) = \int_0^\infty \frac{G(\tau_c)\tau_c}{1 + \omega^2\tau_c^2}\, d\tau_c \tag{18}$$

where

$$\int_0^\infty G(\tau_c)d\tau_c = 1 \tag{19}$$

Of the many possible distribution functions[68-74] only the spectral densities for three (Cole-Cole, Monnerie diamond lattice and log-χ^2)[69-71] and their derivatives will be given.

Each distribution yields quantitatively similar results when applied to a common data set especially if the experimental data are obtained at a single field.[71] Under these circumstances, choosing the model which best describes polymeric dynamics is somewhat arbitrary. The pros and cons of these three functions will be briefly discussed below. It is important, however, to

(68)(a) T. M. Connor, Trans. Faraday Soc., 60, 1574 (1964); (b) J. Mikayke, J. Polymer Science, 28, 477 (1958).

(69)K. S. Cole and R. H. Cole, J. Chem. Phys., 9, 341 (1944).

(70)J. Schaefer, Macromolecules, 6, 882 (1973).

(71)F. Heatley and A. Begum, Polymer, 16, 399 (1976).

(72)R. M. Fuoss and H. G. Kirkwood, J. Am. Chem. Soc., 63, 385(1941).

(73)D. W. Davidson and R. H. Cole, J. Chem. Phys., 18, 1417 (1950); 19, 1484 (1951).

(74)F. Noack, NMR Basic Princ. and Progress, 3, 1971.

examine the general consequences of adopting this type of model for the behavior of the backbone carbon molecular dynamics. Many of the trends experimentally determined for the sidechain carbons are intimately linked to the model chosen for the backbone carbons.

Use of a distribution results in the prediction of frequency-dependent relaxation times over a very wide range of correlation times, including those within the so-called extreme narrowing region predicted from a single correlation time model.[68-71] Thus, very long relaxation times can be field dependent. Measurements made (and conclusions drawn) in such cases may be quite misleading if only one magnetic field is used. NOE's also exhibit more complex behavior relative to that from single correlation time models. A decrease in the NOE can be observed at shorter correlation times, while an increase in the NOE is obtained at longer correlation times depending on the width of the distribution.[70-71] Therefore, carbons exhibiting long, but still frequency dependent T_1's may have unexpectedly low NOE's. Conversely, carbons with very long correlation times may have abnormally high NOE's. It should be noted that, as in the single correlation time model, a given NOE is associated with only one correlation time.

The position of the T_1 minimum for a given carbon as a function of motion (temperature) is also affected by the width of the distribution of correlation times especially for broader distributions (as in the log-χ^2 model).[70] In addition, the curves for T_1 and NOE as a function of correlation times become more shallow as the width of the distribution increases. This is illustrated in Figures 20 and 21 for the log-χ^2 distribution. As a result (for a constant distribution width) the observed temperature dependence of the T_1's and NOE's may be small, particularly for very broad distributions. For cases in which the distribution width varies with temperature, the derivation of a 'simple' activation energy for the polymer becomes impossible.[75]

The spectral densities for the simple distribution functions are as follows:

Cole-Cole Distribution[69-71]

The spectral density function is given by:

$$J_i(\omega) = \frac{1}{2\omega}\left[\frac{\cos[(1-\gamma)\pi/2]}{\cosh(\gamma \ln \omega\tau) + \sin[(1-\gamma)\pi/2]}\right] \tag{20}$$

where γ is the width parameter and may take on any value in the range 0 to 1.0. In the limit $\gamma=1$ the expression for T_1 (and NOE) reduces to essentially the single correlation time model. The

(75) R. MacDonald, J. Chem. Phys., 36, 345 (1962).

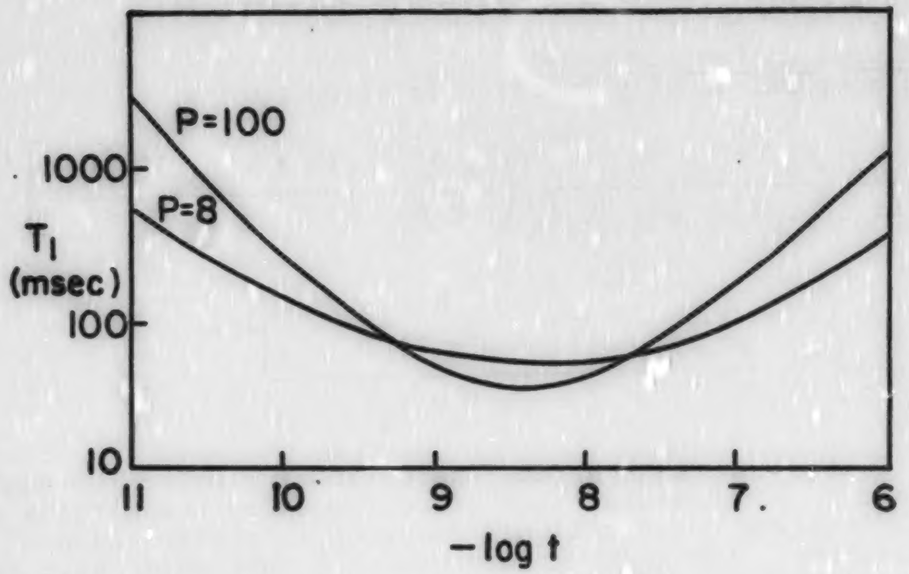

FIGURE 20. Spin-lattice relaxation time, T_1, as a function of correlation time, $\bar{\tau}$ and distribution width, p, for the log-χ^2 distribution (22.6 MHz).

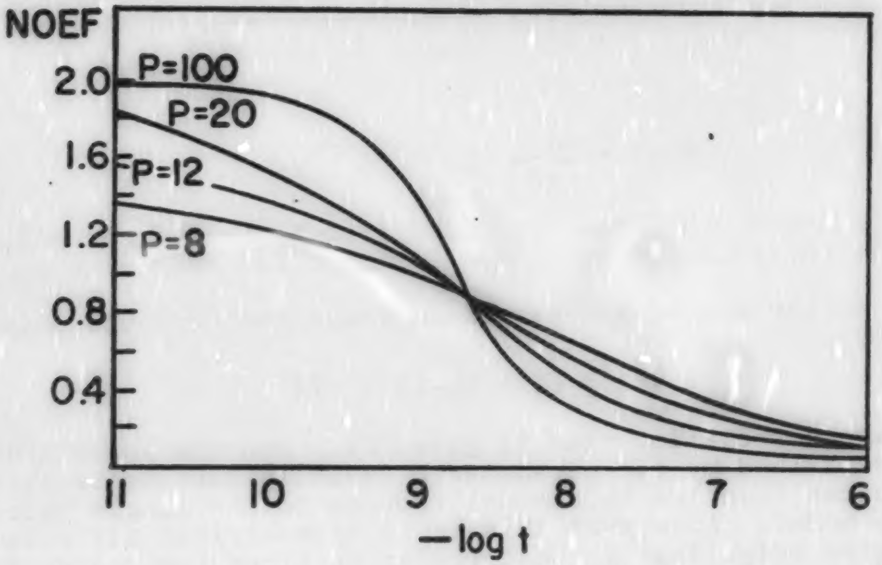

FIGURE 21. Nuclear Overhauser enhancement factor, NOEF, as a function of correlation time and distribution width for the log-χ^2 distribution (22.6 MHz).

Cole-Cole distribution is a symmetrical distribution.

Monnerie Diamond Lattice Model[71]

The spectral density function is given by:

$$J_i(\omega) = \frac{\tau_o\tau_D\ (\tau_o - \tau_D)}{(\tau_o - \tau_D)^2 + \omega^2\tau_o{}^2\tau_d{}^2}\left\{\left(\frac{\tau_o}{2\tau_D}\right)^{1/2}\left[\frac{(1 + \omega^2\tau_o{}^2)^{1/2} + 1}{1 + \omega^2\tau_o{}^2}\right]^{1/2}\right.$$

$$\left.\left(\frac{\tau_o}{2\tau_D}\right)^{1/2}\ \frac{\omega\tau_o\tau_D}{\tau_o - \tau_D}\left[\frac{(1 + \omega^2\tau_o{}^2)^{1/2} - 1}{1 + \omega^2\tau_o{}^2}\right]^{1/2}\ -1\right\} \tag{21}$$

where τ_o is the correlation time characterizing molecular tumbling motions and τ_D is characteristic of conformation transitions since the model involves conformational jumps of a polymer chain on a diamong lattice. For τ_D/τ_o greater than 10 this model also reduces to the single correlation time results.

Log-χ^2 Distribution[70,71]

The spectral density function is given by:

$$J_i(\omega) = \int_o^\infty \frac{\tau\ H(s)(\exp_b s-1)}{(b-1)\{1 + \omega^2\bar{\tau}^2[(\exp_b s-1)/(b-1)2^2\}}\, ds \tag{22}$$

where

$$H(s) = \frac{1}{\Gamma(p)}\,(ps)^{p-1}e^{-ps}p \tag{23}$$

in (23) is the width parameter and $\Gamma(p)$ (which is a normalization factor) is the value of the gamma function for the value p.

Due to the use of a logarithmic scale the variable s is defined by:

$$s = \log_b[1 + (b-1)\ \tau_c/\bar{\tau}] \tag{24}$$

The average correlation time is given by $\bar{\tau}$ and the logarithmic base is described by the parameter b (usually take to be 1,000). For p greater than 100 this model reduces to the single correlation time model. Note that this is an asymmetrical distribution with greater weighting of the correlation times for longer τ values.[70]

Log-χ^2 Distribution Including 'Simple' Internal Rotation[71]

The first modification to be made involves inclusion of internal rotation in the equations of the log-χ^2 distribution in anticipation that such a correction may better describe the motion of the side-chains. The internal motion is incorporated under the following assumptions: (1) only one extra degree of freedome is involved and (2) the carbon in question is assumed to experience a three-fold barrier to rotation. In addition, it can be assumed that the motion of the substituent is either dependent on or independent of the motion of the backbone. For this reason the spectral densities are given in two parts.

1. Dependent Internal Rotation

The spectral density function is given by:

$$J_i(\omega) = \int_0^\infty H(s) \left[\frac{1}{4}(1-3\cos^2\alpha)^2 \frac{\bar{\tau}\left(\frac{b^s-1}{b-1}\right)}{1 + \omega^2\bar{\tau}^2\left(\frac{b^s-1}{b-1}\right)^2} \right.$$

$$\left. 3(\sin^2 2\alpha + \sin^4\alpha) \frac{\left(\frac{2K}{2K+3}\right)\bar{\tau}\left(\frac{b^s-1}{b-1}\right)}{1 + \omega^2\left(\frac{2K}{2K+3}\right)^2 \bar{\tau}^2\left(\frac{b^s-1}{b-1}\right)^2} \right] ds \qquad (25)$$

where

$$K = \tau_g/\tau_c \qquad (26)$$

and

where K is a constant, τ_g is the correlation time for internal rotation and α is the angle between the CH vector and the rotation axis.

2. Independent Internal Rotation[71]

For independent internal rotation the spectral density function is:

$$J_i(\omega) = \int_0^\infty H(s) \left[\frac{1}{4}(1-3\cos^2\alpha)^2 \frac{\bar{\tau}\left(\frac{b^s-1}{b-1}\right)}{1 + \omega^2\bar{\tau}^2\left(\frac{b^s-1}{b-1}\right)^2} + 3(\sin^2 2\alpha + \sin^4\alpha) \right.$$

$$\left. \left[\frac{\tau_g\, \bar{\tau}(b^s-1)}{\bar{\tau}(b^s-1) + \tau_g(b-1)}\right] \Bigg/ \left(1 + \omega^2\left(\frac{\tau\, \tau_g(b^s-1)}{\bar{\tau}(b^s-1) + \tau_g(b-1)}\right)^2\right) \right] ds \qquad (27)$$

Log-χ^2 Distribution Including Multiple Internal Rotations

The final change involves incorporating multiple internal rotations into the dynamics of the sidechain carbons while maintaining the distribution of correlation times for the backbone carbons.

The theory behind derivation of the spectral density functions for the multiple internal rotations has been described in previous papers[60-62] and only the essential equations relevant to the present discussion will be given here.

The spectral density functions for internal rotation alone are given by:[60-62]

$$J_i(\omega) = \sum_{a,b,\ldots,i} |d_{ab}(\beta_a)|^2 |d_{bc}(\beta_b)|^2 \ldots |d_{ni}(\beta_n)|^2 |d_{io}(\beta_i)|^2 \frac{\tau}{1 + \omega^2\tau^2} \tag{28}$$

where

$$\tau = (6D_o + a^2D_a + b^2D_b + \ldots + i^2D_i)^{-1} \tag{29}$$

and D_o is the overall (isotropic) rotational diffusion constant for the molecule, D_a, D_b, ... D_i are the rotational diffusion constants for the carbon-carbon bonds in the alkyl chain; and the d_{ij} are the reduced second order Wigner rotation matrices. The angles, β_a, β_b, ... are the angles between the final axis of rotation and the dipole-dipole vector between the coupled nuclei under investigation.

London and Avitabile[70] have shown that the problem may be considerably simplified, the resulting spectral densities being given by:

$$J_i(\omega) = \sum_{a,b,\ldots,i} B_{ab}B_{bc}\ldots B_{hi}B_{io} \frac{\tau}{1 + \omega^2\tau^2} \tag{30}$$

where the B matrix elements are geometric factors describing the alkyl chain (their values can be found in reference 62).

Rather than refer to these papers individually the above theory of multiple internal rotations developed by Wallach,[59] Levine[60,61] and London[62] will be referred to collectively as the WLL theory.

We propose that the present theory is unsatisfactory for describing the frequency dependent dynamic parameters (T_1, NOE) of the sidechain carbons attached to "macromolecules" whose overall molecular motion must be described by a distribution of correlation times. The extensive data obtained will allow a rigorous comparison of these theories to be made.

We have, therefore, extended the present WLL theory to the situation in which the presence of a distribution of correlation times is required for the backbone carbons. This is accomplished by applying the probability density function for the log-χ^2 distribution (equation 22) to the spectral density of (equation 28).

Of the possible choices of distributions upon which one could expand the model for sidechain dynamics, the log-χ^2 distribution model[70] was chosen. All the models suffer from various deficiencies, however. The Cole-Cole[69,71] is a symmetrical distribution while the asymmetrical log-χ^2 model weights the longer correlation times to be expected in polymeric systems. It should be noted that there is no particular advantage in using the asymmetric log-χ^2 distribution for descriptions of systems characterized by relatively narrow distributions. It can be shown that the χ^2 distribution can be approximated very closely by a normal (i.e., symmetric) distribution for cases in which the number of degrees of freedom is approximately 45 or greater. The most serious deficiency of the Monnerie diamond lattice model is the erratic temperature dependence of τ_D/τ_o for comparable polymers and the physical basis of the model has been questioned.[71] The log-χ^2 model suffers from the presence of the parameter b which must be judiciously chosen so that a wide range of data can be examined by a change in width parameter, p, only. The model breaks down for cases in which $p<\ln b$.

Levine et al.[60,61] have shown that the decay of the autocorrelation functions for carbons more than five bonds removed from a motional restriction such as that imposed by a " macromolecule ", is not affected by varying the diffusion constant of the macromolecule. Thus the T_1's of those carbons are predicted to be independent of the motion of the macromolecule.

Levine[76] noted that such calculations ignore steric hindrance and conformational interdependencies along such a chain. He suggested a more realistic model which incorporated a Monte Carlo approach to the calculation of the time evolution of allowed conformations and an appropriate statistical transition matrix to determine the probabilities of conformational changes. A particularly strong correlation in motions for pairs of adjacent C-H vectors along a chain can be induced (theoretically) by an appropriate choice of the parameter describing the population ratio of the allowed conformations, in conjunction with the introduction of forbidden conformations. This correlation exists for at least the first six pairs of C-H vectors assuming that the potential energy well profiles for different chain segments are not perturbed by differential intermolecular interactions of significance.

Thus the possibility of long range ordering of molecular motions is not excluded from the present theory rather the facts

(76) Y. K. Levine, J. Magn. Resonance, 11, 421 (1973).

point more to the conclusion that these long range 'cooperative' motions have eluded detection. This emphasizes the need for multi-frequency T_1 and NOE measurements for the accurate interpretation of dynamics in polymeric and other complex molecular systems.

Recently, Yasukawa et al.[77] have simulated the random motions of an n-hexyl chain bound to a macromolecule (poly(n-hexyl-4-vinyl pyridinium bromide)) by Monte Carlo methods. Different models were tested according to the transition probabilities chosen for the conformational interconversions. They found that the spectral density functions for the main chain agreed well with the conventional spectral density approximation $[2\tau/(1+\omega^2\tau_c^2)]$ but that the functions for the hexyl chain could not be represented by the same expression.

While a satisfactory fit to the experimental T_1 values was obtained, no mention was made of the predictive value of the theory as applied to the NOE's or changes in frequency.

Numerical Results

Figure 22 illustrates the trends exhibited for the various carbons of an alkyl chain which is described by equal internal rotational diffusion constants ($D_i=1.0 \times 10^{11}$ sec^{-1}) about each bond, the chain being attached to a macromolecule (defined as carbon zero) with an isotropic correlation time of 1.0×10^{-10}sec.

When the overall molecular correlation time ($\bar{\tau}_{mol}$) is longer than the correlation time for internal rotation, the relaxation times increase dramatically along the chain (subject, of course, to the D_i's being constant along the chain). However, the relative NT_1 differences for these carbons are attenuated considerably by the presence of a distribution of correlation times for the backbone carbons, until finally for a broad distribution (e.g., p=8), the NT_1's change very little over the length of the chain. The same effect occurs when the internal rotational diffusion constant is slower than the overall motion.[78] The presence of a distribution can be distinguished from the latter situation from the frequency dependence of the T_1's as well as from certain trends in the NOEF's, as discussed in the following paragraphs.

There is only a slight frequency dependence for the T_1's near the end of the chain with a narrow distribition (p=50); that dependence increases considerably for broader distributions and is present even for the end methyls of long chains for the broad distributions. As the trends indicate, the frequency dependence

---

(78) R. Deslauriers and R. L. Somorjai, J. Am. Chem. Soc., 98, 1931 (1976).

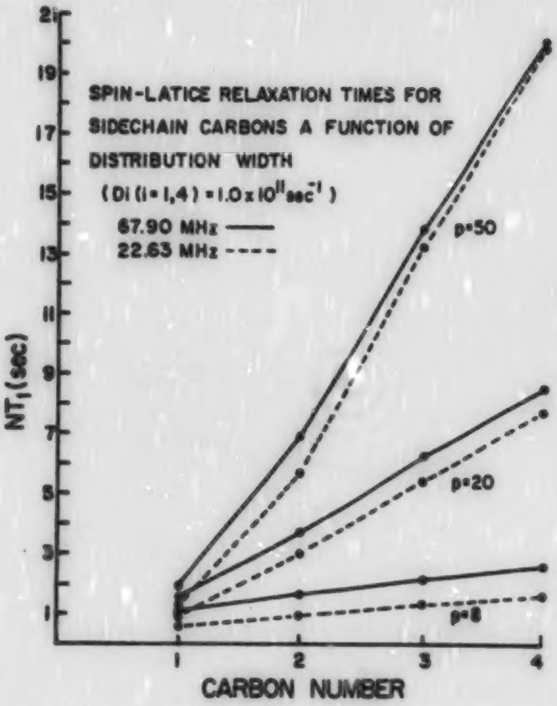

FIGURE 22. Spin-Lattice Relaxation Times for Sidechain Carbons A Function of Distribution Width

disappears entirely for sidechain carbons attached to a backbone whose motion can be described by a single correlation time model. The presence of the distribution lowers T_1's for the sidechain carbons relative to the values calculated for the single correlation time model for identical diffusion constants. Also apparent is the fact that a change in the width of the distribution can induce a large change in the T_1's.

Figure 23 illustrates the effects on the nuclear Overhauser enhancement factor, NOEF, assuming the parameters given in Figure 22.

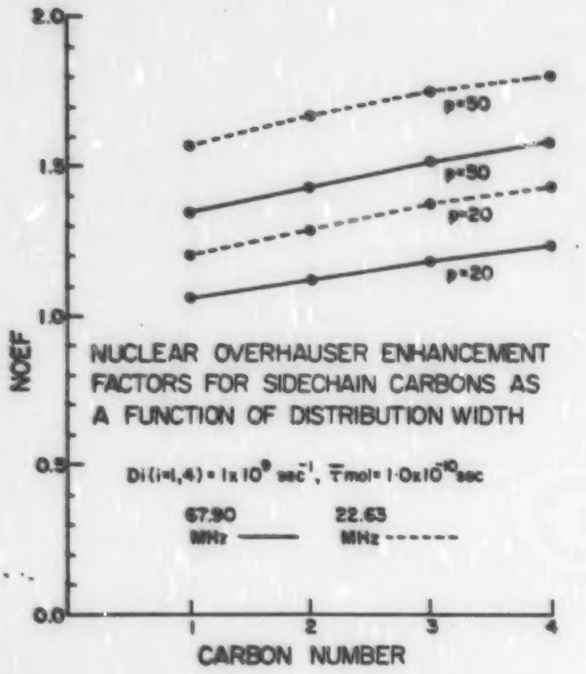

FIGURE 23. Nuclear Overhauser Enhancement Factors For Sidechain Carbons As A Function of Distribution Width

The NOEF's range from 1.2 to 1.5 for C-1 under the given conditions at both fields and increase for the remaining carbons in the chain. For p=50, however, the NOEF is substantial and might be considered maximized within experimental error (depending on the accuracy of the experiment). For very broad distributions the NOEF value is quite low, even for C-4 with a value of approximately 1.4. In general, for most distribution widths, there is only a slight frequency dependence of the NOEF.

The other common situation is depicted by Figures 24 and 25. The rotational diffusion constants along the chain have been reduced by two orders of magnitude so that the internal motion is now comparable to the overall or polymer backbone segmental molecular motion. As has been noted and as shown in Figure 24, there is only a small gradation in the relaxation times along the

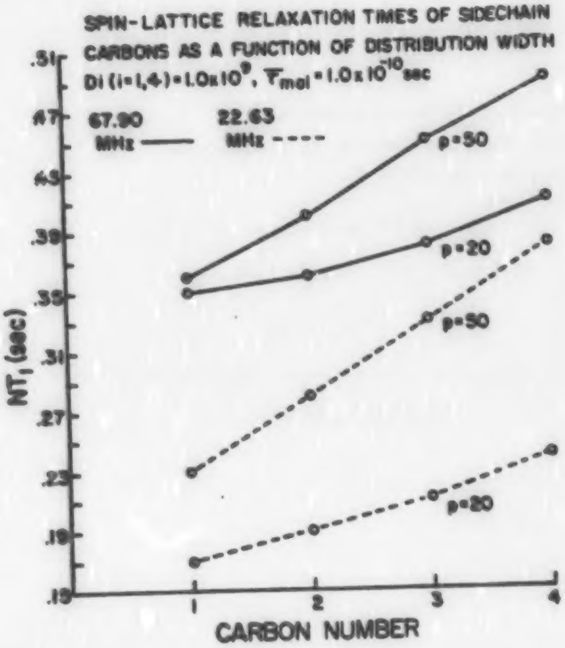

FIGURE 24. Spin-lattice relaxation times of sidechain carbons as a function of distribution width. All diffusion constants are equal along the chain with a value of D_i= 1 x 10^9 sec^{-1} for 67.905 MHz (——) and 22.635 MHz (----). Backbone (carbons) isotropic correlation time is 1. x 10^{-10} sec.

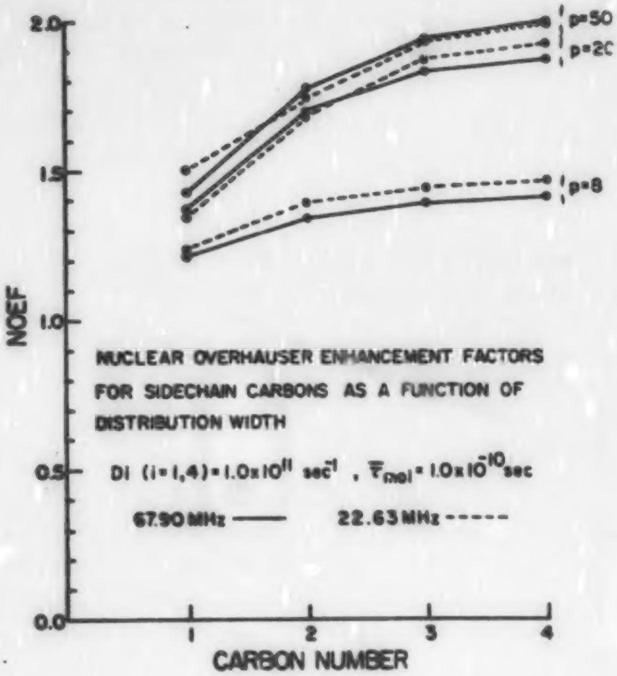

FIGURE 25. Nuclear Overhauser enhancement factors for sidechain carbons as a function of distribution width. Conditions the same as for Fig. 24.

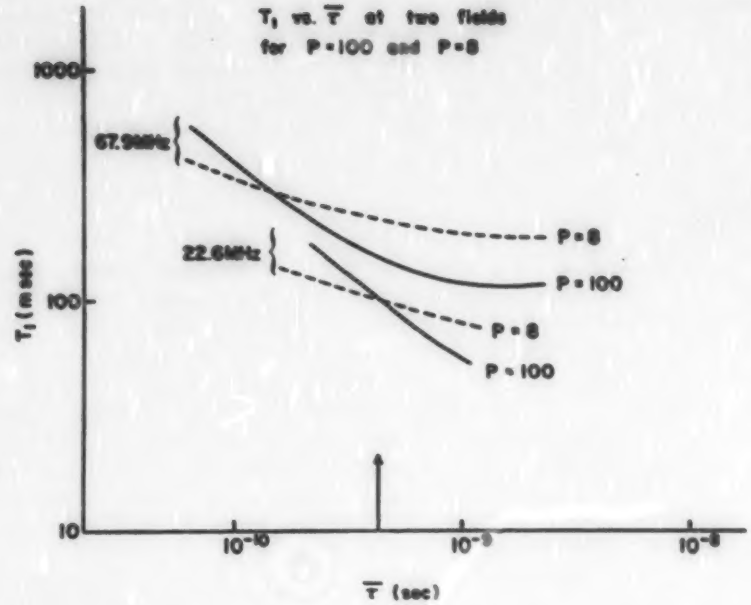

FIGURE 26. Spin-lattice relaxation time versus correlation time for distribution widths of p = 8(----) and p = 100(——) for 67.905 MHz and 22.635 MHz.

sidechain. When internal motions are much slower than the overall molecular motion there would be virtually no change in the T_1's along the chain. In relative terms there is a substantial frequency dependence which, as expected, increases for the broader distribution.

When $\tau_{int} < \tau_{mol}$ the T_1's experience a greater frequency dependence than for the case $\tau_{int} < \tau_{mol}$.

The effects of these parameters on the NOEF's are substantial. The motion results in a larger frequency dependence compared with D_i=1.0 x 10^9 and p=20 the C-4 carbon NOEF is 1.2-1.4 at the two fields, whereas, for D_i=1.0 x 10^{11} sec^{-1} a much broader distribution (p=8) was required to attain comparable NOEF values. The effect of the distribution width is enhanced also. Changing from p=20 to p=50 for D_i=1.0 x 10^9 sec^{-1} results in an NOEF change of 0.35 - 0.4. The same change in p when D_i=1.0 x 10^{11} sec^{-1} affects the NOEF for C-4 by only 1.0.

Two Fields

Heatley and Begum[71] noted that the model parameters should be dependent on the nmr parameters if they are to be calculated with accuracy. The areas which are least sensitive, in general (but not always) are the region of the T_1 maximum and the long correlation time region for the NOEF. In these cases the experimental data (within the limits imposed also by experimental accuracy) are, therefore, reproduced by a number of different model parameters. This ambiguity is alleviated by the use of two fields as widely separated as possible. Three (or more magnetic field strengths) would be even more advantageous. Figure 26 illustrates that a simple frequency measurement of T_1 can lead to the prediction that any distribution width (up to and including the possibility that no distribution exists) will reproduce the experimental T_1 for certain correlation times. The unequivocal statement that a distribution of correlation times is not required for data obtained at only one frequency can now be seen to be an extremely misleading supposition.

Examination of the T_1 data presented in Tables 10-13 reveals several characteristic trends. The T_1's for the sidechain carbons generally increase as a function of distance from the backbone. This is not unexpected, since the same behavior is observed in smaller molecular systems having aliphatic chains effectively anchored at one end because of the presence of a relatively immobile functional group or because of ionic or bonding interactions between the molecule and its immediate environment.[45,61,79,80]

---

(79) D. Doddrell and A. Allerhand, *J. Am. Chem. Soc.*, **93**. ;558 (1971).

In the absence of such a situation, NT_1 values generally increase with distance from the center of mass.[61,80-82] Since motional restriction is greater for the carbon positions closer to the restricting group, correlation times describing these positions should be longer than for carbons removed from the site of restriction. The motions along the aliphatic sidechains of PBMA and PHMA are predominantly characterized by apparent correlation times to the left of the T_1 minimum. Note, however, that the T_1 values for C-3 sometimes show a slight decrease with respect to the T_1 values for C-1 and C-3 at lower temperatures and at the higher field strength.

The most surprising fact is that there is a consistently large field dependence associated with the T_1's of the sidechain carbons. Simple theory [48-49] predicts that the dipolar T_1 of any carbon is independent of the magnetic field strength if the correlation time describing its motion is within the extreme narrowing region $[(\omega_C+\omega_H)^2\tau_c^2<<1]$.

With the exception of C-1, for each sidechain carbon an increase in temperature results in an increase in T_1. The C-1 T_1 values remain relatively static over the wide temperature range studies (~100°) and give evidence for shallow T_1 minimum (particularly for PBMA).

As the temperature is increased, the backbone methylene carbon in PBMA shows a definite T_1 minimum at each magnetic field, while T_1 for the main chain CH_2 carbon of PHMA monotonically increases over the same range. This difference may originate from the fact that, for comparable temperatures, PHMA is further above its glass transition temperature[83] and hence has relatively more freedom of motion.

The minima observed for PBMA (50% w/w toluene-d_8), shown in Table 10, also prove interesting. The backbone CH_2 T_1 minimum is found at ca. 56°C at 22.6 MHz but at ca. 77°C at 67.9 MHz. This is consistent with the fact that the T_1 minimum for the 67.9 MHz magnetic field strength occurs at a shorter correlation time than for the 22.6 MHz field strength. This implies that a greater temperature would be required at higher field strengths to observe the T_1 minimum. The same trend is observed for the quaternary backbone carbon of PBMA.

(81) N.J.M. Birdsall, A.G. Lee, Y.K. Levine, J.C. Metcalfe, P. Partington and G.C.K. Roberts, J.C.S. Chem. Comm. 757 (1973).

(82) C. Chachaty, Z. Wolkowski, F. Pirious and G. Lukacs, Chem. Comm. 951 (1973).

(83) S. S. Rogers and L. Mandelkern, J. Chem. Phys., 61, 985 (1957); J. D. Ferry, "Viscoelastic Properties of Polymers", Wiley, New York, 1961.

TABLE 10. ^{13}C SPIN-LATTICE RELAXATION TIMES OF POLY(BUTYL METHACRYLATE) IN 50%(W/W) SOLUTION IN TOLUENE-D_8

			T_1 (sec)[a]				
Temp. (°C)	C-1	C-2	C-3	C-4	C-CH_3	C-CH_2	C-CR_4
-5	0.27	0.20	0.35	0.93	0.053	----	2.7
6	0.35	0.23	0.39	1.0	0.057	0.21	2.3
21	0.35	0.37	0.73	1.7	0.062	0.17	2.3
46	0.33	0.57	1.2	2.4	0.081	0.12	1.8
55	0.33	0.69	1.5	2.9	0.11	0.098	1.7
75	0.28	0.79	1.5	3.4	0.15	0.085	1.5
80	0.29	0.90	2.5	3.8	0.14	0.086	1.4
93	0.31	0.95	2.7	4.0	0.18	0.093	1.3
98	0.32	1.1	2.8	4.3	0.18	0.094	1.5
111	0.35	1.4	3.4	6.2	0.26	0.11	1.6

[a] Performed at 67.9 MHz

			T_1 (sec)[a]				
Temp. (°C)	C-1	C-2	C-3	C-4	C-CH_3	C-CH_2	C-CR_4
10	0.13	0.20	0.45	1.1	0.025	----	0.69
22	0.11	0.25	0.52	1.3	0.030	0.034	0.64
37	0.093	0.27	0.70	1.5	0.033	0.031	0.56
49	0.094	0.33	0.89	1.7	0.048	0.031	0.54
66	0.085	0.37	0.95	1.8	0.059	0.030	0.49
83	0.10	0.45	1.1	2.1	0.079	0.035	0.53
105	0.15	0.67	1.4	2.8	0.13	0.043	0.70

[a] Performed at 22.6 Mhz

TABLE 11. ^{13}C SPIN-LATTICE RELAXATION TIMES OF POLY(HEXYL METHACRYLATE) IN 50%(W/W) SOLUTION IN TOLUENE-D_8

	T_1 (sec)[a]								
Temp. (°C)	C-1	C-2	C-3	C-4	C-5	C-6	C-CH_3	C-CH_2	C-CR_4
3	0.32	0.21	0.30	0.57	0.81	1.5	0.069	0.32	2.9
34	0.30	0.30	0.55	1.1	1.7	2.6	0.068	0.13	1.8
49	0.31	0.47	0.85	1.6	2.4	3.7	0.092	0.11	1.6
63	0.31	0.54	1.1	2.1	3.2	4.6	0.10	0.097	1.6
83	0.30	0.65	1.4	2.3	3.7	5.3	0.12	0.090	1.5
100	0.31	0.81	1.8	2.9	5.1	7.1	0.22	0.093	1.4

[a] Performed at 67.9 MHz

	T_1 (sec)[a]								
Temp. (°C)	C-1	C-2	C-3	C-4	C-5	C-6	C-CH_2	C-CH_3	C-CR_4
17	0.12	0.14	0.26	0.47	0.75	1.6	0.024	-----	0.63
43	0.11	0.24	0.47	0.90	1.5	2.3	0.037	0.035	0.54
64	0.10	0.28	0.63	1.1	2.1	3.3	0.057	0.029	0.40
74	0.098	0.36	0.83	1.5	2.5	4.2	0.073	0.028	0.46
89	0.10	0.38	0.95	1.7	3.0	4.8	0.086	0.031	0.47
102	0.13	0.52	1.0	1.8	3.3	5.1	0.14	0.042	0.58

[a] Performed at 22.6 MHz

TABLE 12. ^{13}C SPIN-LATTICE RELAXATION TIMES OF POLY(BUTYL METHACRYLATE) IN 50%(W/W) SOLUTION IN BENZENE-D_6

	T_1(sec)[a]						
Temp. (°C)	C-1	C-2	C-3	C-4	C-CH_3	C-CH_2[c]	C-CR_4
10	0.41	0.30	0.51	1.2	0.065	----	2.5
22	0.39	0.38	0.67	1.7	0.069	0.19	2.3
31	0.46	0.51	1.0	2.3	0.076	0.17	2.4
40	0.41	0.53	1.1	2.4	0.078	0.13	2.1
50	0.26	0.65	1.4	2.7	0.088	0.11	1.9

[a] At 67.9 MHz, estimated maximum error ± 10% typical error ≳ 5% (see text)

[b] Temperature ± 2°C

[c] At low temperature, unable to calculate T_1 due to peak broadening

TABLE 13. ^{13}C SPIN-LATTICE RELAXATION TIMES OF POLY(HEXYL METHACRYLATE) in 20%(W/W) SOLUTION IN TOLUENE-D_8

	T_1 (sec)[a]								
Temp. (°C)	C-1	C-2	C-3	C-4	C-5	C-6	C-CH_3	C-CH_2	C-CR_4
16	0.26	0.27	0.54	0.87	1.4	2.1	0.049	0.084	1.6
22	0.25	0.28	0.55	1.0	1.5	2.4	0.057	0.079	1.3
35	0.24	0.35	0.67	1.2	2.0	2.8	0.060	0.063	1.2
65	0.30	0.60	1.4	2.4	3.6	4.3	0.099	0.067	1.2
91	0.37	0.92	2.0	4.2	5.0	6.8	0.18	0.081	1.5

[a] Performed at 67.9 MHz

A minimum is observed for PHMA (50% w/w in toluene-d_8) at 22.6 MHz, as can be seen from the data in Table 11. Observation of a minimum at the higher field strength, requires temperatures unattainable in toluene-d_8. A more dilute solution of PHMA (20% w/w in toluene-d_8) does exhibit a minimum at approximately 50°C.

Table 14 contains the nuclear Overhauser enhancement factors for PBMA. At low temperatures, the NOEF's for the sidechain carbons become equal near the theoretical maximum value of 2. As the temperature is increased, the NOEF for C-1 decreases considerably (by a factor of _ca._ 5) while the C-2 and C-4 NOEF values decrease much less (by a factor of _ca._ 2). The NOEF difference between C-1 and C-2 increases as the temperature increases while the C-2 and C-4 difference remains relatively constant. The backbone methylene NOEF also decreases somewhat with temperature. At 101°C it reaches an NOEF which is comparable to that observed for C-1 sidechain. The backbone methyl substituent NOEF increases with temperature by a factor of 2 over the range 14°-101°C.

The situation is somewhat different for the low field data. The C-1 NOEF increases with temperature while the C-2 and C-4 NOEF values remain relatively constant over the temperature range, but at lower than the maximum permissible value. At high temperatures, the NOEF's for the sidechain carbons tend to equalize. A small increase in NOEF with temperature is noted for both the backbone carbons.

C-CH_3

The trends exhibited by the methyl group directly attached to the backbone can be reproduced by a model which incorporates dependent internal rotation of the substituent attached to a backbone whose overall molecular motion must be described by a distribution of correlation times.

Figure 27 illustrates that the T_1 and NOEF should increase with increasing temperature for the calculated backbone correlation times for the various temperatures studied.

Previous studies on related methyl groups have pointedly illustrated the varied behavior of these substituents. The correlation time of the methyl group in poly(propylene oxide) was found to be independent of the average correlation time of the backbone while the methyl in poly(isobutylene) exhibits an internal correlation time which is proportional to the backbone correlation time. This is similar to the situation for poly(methyl methacrylate).

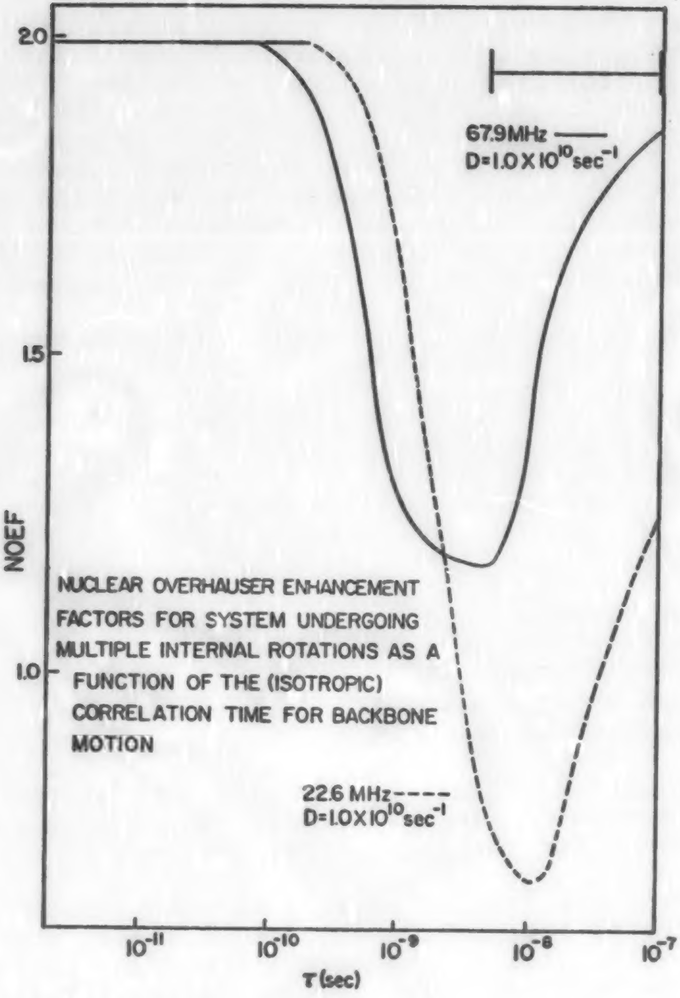

FIGURE 27. Nuclear Overhauser enhancement factors for a system undergoing multiple internal rotations.

TABLE 14. NUCLEAR OVERHAUSER ENHANCEMENTS FOR POLY(BUTYL METHACRYLATE) IN 50%(W/W) SOLUTION IN TOLUENE-D_8

		NOEF[a] [b]					
Temp. (°C)	C-1	C-2	C-3[c]	C-4	C-CH_3	C-CH_2	C-CR_4
-5	2.0	1.9	---	2.0	----	----	0.51
14	1.4	1.7	---	1.8	0.71	0.67	0.47
34	0.81	1.6	---	1.6	0.83	0.56	0.61
42	1.1	1.6	---	1.5	1.2	0.43	0.66
52	0.80	1.4	---	1.5	1.2	0.44	0.50
64	0.61	1.3	---	1.4	1.3	0.44	0.59
80	0.54	1.3	---	1.3	1.3	0.43	0.56
101	0.42	0.98	---	1.3	1.4	0.36	0.59

[a] At 67.9 MHz, estimated maximum error ± 10%

[b] NOE = NOEF + 1, therefore $NOEF_{max}$ = 1.988

		NOEF[a]					
Temp. (°C)	C-1	C-2	C-3[c]	C-4	C-CH_3[b]	C-CH_2	C-CR_4
11	0.47	1.5	---	1.6	0.99	---	0.89
21	0.54	1.7	---	1.7	---	0.30	0.88
31	0.23	1.0	---	1.2	0.91	0.30	0.22
50	0.69	1.2	---	1.6	1.8	0.40	0.68
63	0.79	1.9	---	1.3	1.3	0.71	0.75
81	0.9	1.1	---	1.4	1.8	0.66	1.3
104	1.1	1.3	---	1.4	1.4	0.59	1.1

[a] Performed at 22.6 MHz

[b] NOEF at 21 °C absent due to apparent large error, (NOEF = 2.21)

[c] NOEF's not determined, overlap with solvent resonances prevents peak integration.

TABLE 15. NUCLEAR OVERHAUSER ENHANCEMENT FACTORS FOR POLY(HEXYL METHACRYLATE) IN 50%(w/w) SOLUTION IN TOLUENE-D_8

Temp(°C)				67.9 MHz					
	C-1	C-2	C-3	C-4	C-5	C-6	C-CH$_3$	C-CH$_2$	C-CR$_4$
3	2.06	1.94	1.66	1.58	1.50	1.62	0.67	--	1.15
17	1.73	1.83	1.62	1.60	1.51	1.66	0.79	0.70	0.81
35	1.21	1.63	1.68	1.64	1.63	1.71	1.09	0.62	0.47
50	1.04	1.57	1.71	1.75	1.75	1.73	1.12	0.27	0.58
66	1.88	1.56	1.80	1.79	1.85	1.94	1.57	0.42	0.64
100	1.79	1.52	1.83	1.89	1.91	1.98	1.76	0.51	0.72

Temp(°C)				22.6 MHz					
	C-1	C-2	C-3	C-4	C-5	C-6	C-CH$_3$	C-CH$_2$	C-CR$_4$
17	0.64	1.67	1.83	1.59	1.91	1.98	0.91	0.41	0.51
44	0.95	1.60	1.72	1.72	1.71	1.80	1.-6	0.33	0.88
66	1.06	1.46	1.28	1.22	1.12	1.31	1.53	0.52	0.58
76	0.87	1.30	1.44	1.32	1.52	1.39	1.04	0.67	0.68
90	0.91	1.07	1.06	1.43	1.15	1.44	1.11	0.-1	0.81
103	1.09	1.25	1.31	1.46	1.19	1.15	1.65	0.52	0.76

C-1 Carbons

No attempt was made to fit all data exactly by systematically varying the p parameter, the diffusion constants or the average correlation times by very small increments. The purpose of the present analysis is the determination of the relative importance of the distribution of correlation times for the backbone carbons with respect to the multiple internal rotations about the C-C bonds. It should suffice to choose parameters which encompass the extremes of measured T_1 and NOE values and hence the extremes of temperature. Numerous parameters have been varied to illustrate their effects and to elucidate whether the trends in the experimental data are satisfactorily reproduced.

Data for the C-1 carbons in both polymers indicate an insensitivity to change in temperature at both fields. In addition there is a great similarity in the magnitude and frequency dependence of the T_1 values when comparing PBMA with PHMA. Considering the changes in correlation times and distribution widths associated with an approximate change in temperature of 100°C the question becomes one of whether the theory can reasonably predict this behavior.

Table 17 summarizes the numerical results for the C-1 carbon with a set of parameters ($\bar{\tau}$, p) chosen from the experimental results for two widely different temperatures. Therefore, the average correlation times span two orders of magnitude with the shorter correlation times (5×10^{-9} sec) being associated with the narrower distribution parameters (p=50 and p=20) while the long correlation time is associated with the broad distribution width (p=8, b=1000 in all cases).

For a large range in distribution widths and correlation times the calculated T_1's at a given field are relatively constant, even allowing for a moderate increase in the internal rotational diffusion constant (D_1) with increasing temperature.

The observed T_1's differ in value by a factor of two to three at the two magnetic field strengths; a trend which can be reproduced with the parameters of Table 17.

The nuclear Overhauser enhancement factors are calculated to be in the range 1.0-1.3 for the given parameters, but inspection of the data reveals that a much wider range of values are observed, as evidenced by the extreme values obtained at the highest and lowest temperatures for both polymers. While the calculated NOEF's are within experimental error of the observed (±0.3η) for most of the intermediate temperatures, the deviations from calculated values at the highest and lowest temperatures are definitely outside of experimental error.

Figure 27 illustrates the fact that for short correlation times (high temperatures) the NOEF at 22.6 MHz is greater than the NOEF at 67.9 MHz. This is the situation one predicts (and observes) for a system which can be described by a single correlation time or a simple distribution of correlation times. However, the more complex behavior observed in the present case can be attributed to the effect of internal rotation superimposed upon the overall molecular motion. Note that as the correlation times increase (as the temperature decreases) the difference between the two magnetic field strengths becomes smaller. Finally, for correlation times longer than $\sim 2.0 \times 10^{-9}$ sec the NOEF at 67.9 MHz becomes greater by a substantial amount; the differences diminishing again for very long correlation times.

The experimental data verify this behavior qualitatively. The NOEF for PBMA at 67.9 MHz and -5°C is at its maximum value (2.0η). As the temperature is increased the trend reverses until at ~100°C the NOEF at 22.6 MHz is greater than that at 67.9 MHz.

Theoretically, the presence of the distribution equalizes the NOEF's but the effects of the internal rotation tend to negate this. The net result is that the present theoretical modification emphasizes the effect of the distribution in a manner contrary to observation at the lowest temperatures.

Anisotropy in the backbone motions can introduce an additional angular factor in the calculations. It has been shown that changing the angle between the first bond and the molecular Z axis (assuming the symmetric rotor model) can affect the relaxation times considerably as a function of the anisotropy. This possibility has not been included in the present calculations and may partially obviate the discrepancies, particularly for C-1 since the effects of anisotropic motion are calculated to be greatest at this chain position.

For a constant diffusion coefficient the WLL theory predicts that the T_1's will increase as the temperature decreases (within the calculated range of correlation times for PBMA and PHMA). While this is not in fact the case, it should be noted that such an insensitivity to temperature may result from the WLL theory provided that the diffusion constants decrease enough to offset the increase due to the longer backbone correlation times.

C-2 Carbons

For similar temperatures the C-2 carbon T_1's of PBMA are larger than the corresponding values of PHMA. This is consistent with the greater motional freedom associated with a shorter chain which lessens the effects of inter- and intra-molecular interactions due to chain entanglements. However, the glass transition temperature of PHMA should be lower than that of PBMA so that direct and absolute comparison of the polymers at similar temperatures is not free of ambiguity as to the origin of the dynamic differences.

The frequency dependence of the T_1's for C-2 is not as great on the average as that observed for C-1 but is still of considerable magnitude and outside experimental error. Inspection of Table 9 in conjunction with Tables 10 and 3 reveals that the distribution-modified internal rotation theory is able to predict the frequency dependent behavior.

The NOEF's (Tables 14 and 15) do not follow the trends that were so obvious for C-1. They tend to average $\sim 1.5 \pm 0.3\eta$ (except for the temperature extremes at 67.9 MHz). Table 18 therefore would indicate that the distribution is relatively broad ($p \leq 20$) and further shows that an increase in p values (i.e., approaching the WLL theory) will result in predicted NOEF's which are consistently larger than the observed values (while also predicting a small or negligible frequency dependence contrary to observation).

Under certain circumstances, the C-2 carbon T_1's of PBMA and PHMA are less than the T_1's of C-1 and C-3 at the same temperature. The effect is greatest for low temperatures and the higher magnetic field strength. Even for 67.9 MHz the effect disappears for temperatures above 20-40°C.

Doddrell et al. have shown that increasing the rate of internal rotation can result in a decrease in T_1 if motion of the backbone carbons satisfies the condition $\omega^2\tau^2 >> 1$ in conjunction with the condition $W^2\tau^2_{eff} \sim 1$ for the sidechain carbon whose T_1 is shortened.

The latter condition is not necessary for observation of the phenomenon. Even for $\omega^2\tau^2_{eff} << 1$ the effect may occur. Levine, et al.[60,61] have proposed the following explanation.

The transformation along the chain decreases the effective correlation time of the slow motion, leading to an increase in the spectral density at high frequencies. For carbon 2 this increase is greater than the concomitant decrease in spectral, density due to the internal rotations. This results in a net increase in spectral density at high frequencies and a reduction in T_1 values.

It was noted that the effect is very sensitive to the Larmor frequencies involved. Thus (at 24kG) the effect was seen for $^1H \ldots {}^1H$ relaxation but not for ^{13}C-^1H relaxation. This is consistent with the fact that the C-2 T_1's only decrease relative to C-1 for the higher field (higher Larmor frequencies) and only at certain temperatures (for which the condition $\omega^2 \tau^2 >> 1$ is satisfied).

C-3 Carbons

Not until one reaches C-3 (see Tables 19 and 20) do the greatest differences in theories become apparent. The WLL theory predicts that a virtually maximum NOEF should be observed for the correlation times spanned by the backbone carbons. In fact, a consistently reproducible NOEF which is less than the maximum value is observed for PHMA. While data are not available for C-3 of PBMA, interpolation from the C-2 and C-4 NOEF's confirm the trends of PHMA. It is not reasonable to expect that the C-3 NOEF's of PBMA could vary greatly from the average values of the C-2 and C-4 NOEF's since the values for these latter carbons are generally so close over the entire temperature range studied.

The frequency dependence of the C-3 T_1's is again considerable for both polymers. Even for p values of 50, one predicts that the frequency dependence is quite small; vanishing for the single correlation time (WLL) theory. The low and intermediate temperature data is reproduced quite reasonably by inclusion of the distribution effects, particularly for PHMA. The frequency dependence of the T_1's for PBMA at high temperatures ($\gtrsim$90°C) cannot be reproduced with a reasonable set of parameters, the backbone distribution is too narrow to accomodate the observed differences.

C-4 Carbons

PBMA

The C-4 carbon of PBMA is (Tables 21 and 22) methyl group and, therefore, direct comparison with the C-4 carbon of PHMA is not possible in the manner chosen for carbons C-1 through C-3. Table 21 specifically illustrates the calculated methyl values for C-4 carbon with the given parameters, hence the corresponding T_1's of Table 10 for PBMA can be compared directly.

The low temperature (less than -50°C) frequency dependence of the T_1's (see Table 22) is reasonably predicted by the present theory, i.e., the T_1's vary by approximately 20% with the change in frequency from 22.6 MHz to 67.9 MHz. At high temperatures the frequency dependence increases in relative magnitude and cannot be quantitatively predicted by this or any other theory presently known.

The implication is that the terminal methyl has associated with it some very long correlation times. The gradual evolution of the frequency dependence under our present theoretical assumptions does not lead to the observed facts. Obviously, factors as yet unaccounted for contribute significantly to the dynamic behavior of the terminal methyl group.

One is reminded at this point of the results of Levine[76] which predicted that a strong correlation in the motions of pairs of C-H vectors on adjacent atoms may be possible. Thus, the C-4 carbon of PBMA could be considered as interacting with the C-3 carbon and acquiring characteristics indicative of the C-3 carbon such as an increased frequency dependence for comparable diffusion coefficients.

The origin of the unusual T_1's of these polymers for C-4 is not reflected in any precipitous changes in nuclear Overhauser enhancement factors at this position. The experimental values are still less than maximum as predicted by distribution widths less than or equal to about $p=20$.

C-5 and C-6 Carbons (PHMA only)

The NOEF's for C-5 are predicted from the relatively broad distribution width associated with the backbone carbon T_1's. As noted in the numerical results section, the relative insensitivity of the NOEF's for broad distributions is predicted to extend quite a distance from carbon 0 for reasonable diffusion coefficients. The same can be said for the C-6 carbons. Despite NT_1 values of the order of 20.0 seconds, the NOEF's are generally less than maximum.

The low temperature C-5 results shown in Table 23 are in accord with theoretical predictions, particularly for temperatures less than 50°C.

Cross Correlation Effects

Cross correlation effects (even under proton decoupled conditions) should be most evident for methylene (or methyl) carbons undergoing anisotropic reorientation with correlation times that are of the order of $\omega_c \sim 6D_o$ where D_o is the diffusion constant for overall motion of the molecule and ω_c is the Larmor frequency of carbon. London et al. have shown that, except for C-1, the effects are insignificant for internal diffusion constants, Di, equal to 10^9 sec^{-1} but became more important for $Di=10^{10}$ sec^{-1} and 10^{11} sec^{-1} and an internal rotational diffusion constant (Di) of $\sim 10^{10}$ sec^{-1}.

The cross correlation effects are attenuated as the carbon under consideration becomes more remote from the site of substitution on the main chain.

Examination of the data in Table 16 shows that the range $D_o = \sim 10^6 - 10^8$ sec^{-1} for the backbone diffusion constant is covered by the temperature changes.

This is precisely the most sensitive region for detection of cross correlation effects. In addition the rotational diffusion constants are of the order of $10^{10} - 10^{11}$ sec^{-1}. The predicted deviation due to cross correlation effects neglecting the effects of a distribution of correlation times, in the NOEF for C-1 and

C-2 under these conditions is approximately 0.2-0.5 units. The data show no evidence for these effects.

Summary and Conclusions

1. Invocation of a distribution of correlation times for the backbone carbons of PHMA and PBMA yields a satisfactory fit of the experimental data at two fields and a variety of temperatures.

2. The single correlation time approximation may be inadequate for describing not only the dynamic behavior of polymer backbone carbons but also the alkyl (or related) sidechain substituents.

3. Carbons which are, strictly speaking, eight bonds removed from the backbone exhibit frequency dependent relaxation times and less than maximum nuclear Overhauser enhancement factors. We have preliminary data on a related polymer, poly-(_n_-octyl acrylate), which indicates that ten bonds are required in these polymers before relatively temperature independent NOEF's are observed.

4. Multiple internal rotation effects alone cannot account for the observed nmr parameters.

5. The distribution of correlation times for the backbone carbons is effective in altering the dynamic parameters of the sidechain carbons, inducing frequency dependent T_1 behavior.

6. The inability to fit the high temperature spin-lattice relaxation times for the terminal (PHMA, PBMA) and penultimate carbons (PHMA) indicates that the present theoretical modifications are insufficient in some respect. The assumptions of independent bond rotations and/or stochastic diffusion may be one source of the discrepancy.

7. Alkyl chain dynamics in various environments, as measured by nmr, require quite different motional models. One model should not even be expected to uniquely determine the nmr parameters in different polymers.

8. Unlike data for the n-alkanes, the relaxation data for these polymers cannot be interpreted by the model in which the diffusion constants for internal rotation are the same for all bonds. The data is better explained in terms of a slower diffusion constant for the first bond and slightly increasing diffusion constants for the remaining carbons. The data for the terminal methyl, however, does require that a large increase in internal rotation about the final bond be invoked.

Studies of hydrocarbon chains in dipalmitoyl lecithin bilayers provide an interesting comparison in that the motions of the chain near the terminal methyl are identical with those of the corresponding n-alkane carbons and in qualitative agreement with the present calculated diffusion constants. The most significant observation is that the motions of the C-C bonds near the glycerol bridge of the lipids are an order of magnitude slower than those of the remaining chain carbons.

It is possible that the slow motions required to fit the observed data may be oscillatory in nature rather than involving a full rotation. Under these circumstances, the correlation time is the product of the true correlation time and a factor describing the amplitude of the oscillatory motion. Unfortunately, it is not possible to distinguish an increase in the true rotational diffusion constant from an increase in the amplitude of oscillation along the chain.

TABLE 16. CORRELATION TIMES, WIDTH PARAMETERS, AND SPECTRAL QUANTITIES FOR PBMA IN TOLUENE -d_8 AS A FUNCTION OF TEMPERATURE AND THE LOG-χ^2 DISTRIBUTION MODEL

Temp. in °C	67.9 MHz				22.7 MHz				$\tau_c(10^9 sec)$	P
	T_1(cal.)	T_1(obs.)	NOEF(cal.)	NOEF(obs.)	T_1(cal.)	T_1(obs.)	NOEF(cal.)	NOEF(obs.)		
100	0.19	0.19	1.37	1.36	.059	.079	1.59	1.59	7.1	20
80	0.17	0.17	1.43	1.43	.051	.069	1.67	1.66	5.0	20
50	0.22	0.22	1.41	1.44	.059	.063	1.59	1.40	11	12
40	0.25	0.25	1.45	1.43	.068	.062	1.61	----	16	8
35	---	0.27	----	1.56	----	.062	----	1.30	-22	<8
20	---	0.34	----	1.63	----	.067	----	1.30	-130	<8

[a] All the observed values are for the methylene backbone carbon (C-CH_2). All T_1 values are in secs. and are equal to 2X the actual or predicted value for this carbon (otherwise known as the NT_1 or the T_1 expected had there only been one proton present.)

TABLE 17. CALCULATED METHYLENE SPIN-LATTICE RELAXATION TIMES AND NUCLEAR OVERHAUSER ENHANCEMENT FACTORS FOR THE C-1 CARBON

	67.9 MHz		22.6 MHz	
Distribution Width[a]	T_1(sec)	NOEF(η)	T_1(sec)	NOEF(η)
P=8 (τ=1.3X10^{-7}sec)				
D_1-1.2	0.24	1.1	0.12	1.1
D_1=3.0	0.34	1.1	0.16	1.1
P=20 ($\bar{\tau}$=5.0X10^{-9}sec)				
D_1=1.2	0.26	1.3	0.14	1.3
D_1=3.0	0.40	1.3	0.21	1.2
P=50 ($\bar{\tau}$=5.0X10^{-9}sec)				
D_1=1.2	0.29	1.3	0.15	1.2
D_1=3.0	0.46	1.2	0.21	1.0

[a] Log-χ^2 distribution assumed; all Di's are given in units of 10^{10} sec^{-1}

TABLE 18. CALCULATED METHYLENE SPIN-LATTICE RELAXATION TIMES AND NUCLEAR OVERHAUSER ENHANCEMENT FACTORS FOR THE C-2 CARBON

	67.9 MHz		22.6 MHz		Experimental Temperature (°C)[b]	
Distribution Width[a]	T_1(sec)	NOEF(η)	T_1(sec)	NOEF(η)	PBMA	PHMA
P=8 ($\bar{\tau}$=1.3X10^{-7}sec)						
D_1=1.2, D_2=3.0	0.36	1.2	0.20	1.3		34
D_1=1.2, D_2=5.0	0.41	1.2	0.22	1.3	21	43
D_1=1.2, D_2=10.0	0.48	1.3	0.26	1.3		
P=20 ($\bar{\tau}$=v.0X10^{-9}sec)						
D_1=1.2, D_2=3.0	0.52	1.6	0.37	1.6	46	63
D_1=1.2, D_2=5.0	0.62	1.6	0.44	1.6	55	83
D_1=1.2, D_2=10.0	0.75	1.6	0.53	1.6		100
P=50 ($\bar{\tau}$=5.0X10^{-9}sec)						
D_1=1.2, D_2=1.0	0.51	1.8	0.40	1.7		
D_1=1.2, D_2=3.0	0.78	1.8	0.60	1.6		
D_1-1.2, D_2=5.0	0.92	1.7	0.69	1.6	98	
D_1=1.2, D_2=10.0	1.13	1.7	0.81	1.5		

[a] Log-χ^2 distribution assumed; all Di's are given in units of 10^{10} sec-1

[b] listed diffusion coefficients reproduce observed data for the stated experimental temperatures

TABLE 19. CALCULATED METHYLENE SPIN-LATTICE RELAXATION TIMES AND NUCLEAR OVERHAUSER ENHANCEMENT FACTORS FOR THE C-3 CARBON

	67.9 MHz		22.6 MHz		Experimental Temperature (°C)[b]	
Distribution Width[a]	T_1(sec)	NOEF(η)	T_1(sec)	NOEF(η)	PBMA	PHMA
P=8 ($\bar{\tau}$=1.3X10^{-7}sec)						
D_1=1.2, D_2=5.0, D_3=5.0	0.59	1.3	0.34	1.4		34
D_1=1.2, D_2=5.0, D_3=7.0	0.63	1.3	0.37	1.4		
D_1=1.2, D_2=5.0, D_3=10.0	0.69	1.3	0.40	1.4	21	43
P=20 ($\bar{\tau}$=5.0X10^{-9}sec)						
D_1=1.2, D_2=5.0, D_3=5.0	1.18	1.7	0.96	1.8	46	63
D_1=1.2, D_2=5.0, D_3=7.0	1.30	1.7	1.08	1.8		83
D_1=1.2, D_2=5.0, D_3=10.0	1.47	1.7	1.21	1.8	55	
P=50 ($\bar{\tau}$-5,0X10^{-9}sec)						
D_1=1.2, D_2=5.0, D_3=5.0	2.20	1.9	2.00	1.9		
D_1=1.2, D_2=5.0, D_3=7.0	2.47	1.9	2.24	1.8		
D_1=1.2, D_2=5.0, D_3=10.0	2.80	1.9	2.51	1.8	98	

[a] Log-χ^2 distribution assumed; all Di's are given in units of 10^{10} sec^{-1}.

[b] Listed diffusion coefficients reproduce observed data for the stated experimental temperatures.

TABLE 20. CALCULATED METHYLENE SPIN-LATTICE RELAXATION TIMES AND NUCLEAR OVERHAUSER ENHANCEMENT FACTORS FOR THE C-3 CARBON

	67.9 MHz		22.6 MHz		Experimental Temperature (°C)[b]
Distribution Width[a]	T_1(sec)	NOEF(η)	T_1(sec)	NOEF(η)	PBMA
P=8 ($\bar{\tau}=1.3\times10^{-7}$sec)					
$D_1=1.2$, $D_2-D_3=10.0$	0.78	1.4	0.46	1.4	21
$D_1=1.2$, $D_2=10.0$, $D_3=30.0$	1.03	1.4	0.62	1.4	37
$D_1=1.2$, $D_2=10.0$, $D_3=70.0$	1.30	1.4	0.79	1.4	46
P=20 ($\bar{\tau}=5.0\times10^{-9}$sec)					
$D_1=1.2$, $D_2=D_3=10.0$	1.80	1.8	1.49	1.8	
$D_1=1.2$, $D_2=10.0$, $D_3=30.0$	2.61	1.7	2.13	1.8	
$D_1=1.2$, $D_2=10.0$, $D_3=70.0$	3.39	1.7	2.70	1.7	
P=50 ($\bar{\tau}=5.0\times10^{-9}$sec)					
$D_1=1.2$, $D_2=D_3=10.0$	3.49	1.9	3.06	1.8	
$D_1=1.2$, $D_2=10.0$, $D_3=30.0$	5.00	1.8	4.18	1.7	
$D_1=1.2$, $D_2=10.0$, $D_3=70.0$	6.24	1.8	5.00	1.7	

[a] Log-χ^2 distribution assumed; all Di's are given in units of 10^{10} sec^{-1}.

[b] Listed diffusion coefficients reproduce observed data for the stated experimental temperatures.

TABLE 21. CALCULATED METHYLENE SPIN-LATTICE RELAXATION TIMES AND NUCLEAR OVERHAUSER ENHANCEMENT FACTORS FOR THE C-4 CARBON

	67.9 MHz		22.6 MHz		Experimental Temperature (°C)[b]
Distribution Width[a]	T_1(sec)	NOEF(η)	T_1(sec)	NOEF(η)	PHMA
P=8 ($\overline{\tau}$=1.3X10^{-7}sec)					
D_1=1.2, D_2=D_3=D_4=D_5=5.0	0.74	1.4	0.44	1.4	
D_1=1.2, D_2=5.0, D_3=7.0, D_4=10.0	0.87	1.4	0.53	1.4	
D_1=1.2, D_2=5.0, D_3=10.0 D_4=30.0	1.18	1.4	0.73	1.4	34
P=20 ($\overline{\tau}$=5.0X10^{-9})					
D_1=1.2, D_2=D_3=D_4=5.0	1.74	1.8	1.61	1.9	49
D_1=1.2, D_2=5.0, D_3=7.0, D_4=30.0	2.28	1.8	2.01	1.9	
D_1=1.2, D_2=5.0, D_3=10.0, D_4=30.0	3.58	1.8	3.19	1.9	
P=50 ($\overline{\tau}$-5.0X10^{-9}sec)					
D_1=1.2, D_2=D_3=D_4=5.0	3.64	2.0	3.56	2.0	
D_1=1.2, D_2=5.0, D_3=7.0, D_4=10.0	4.95	2.0	4.82	2.0	
D_1=1.2, D_2=5.0, D_3=10.0 D_4=30.0	7.98	2.0	7.68	2.0	

[a] Log-χ^2 distribution assumed; all Di's are given in units of 10^{10} sec^{-1}.

[b] Listed diffusion coefficients reproduce observed data for the stated experimental temperatures.

TABLE 22. CALCULATED METHYL SPIN-LATTICE RELAXATION TIMES AND NUCLEAR OVERHAUSER ENHANCEMENT FACTORS FOR THE C-4 CARBON

	67.9 MHz		22.6 MHz		Experimental Temperature (°C)[b]
Distribution Width[a]	T_1(sec)	NOEF(η)	T_1(sec)	NOEF(η)	PBMA
p=8 ($\bar{\tau}=1.3\times10^{-7}$ sec)					
$D_1=1.2$, $D_2=5.0$, $D_3=10.0$, $D_4=30.0$	0.79	1.4	0.49	1.4	
$D_1=1.2$, $D_2=10.0$, $D_3=10.0$, $D_4=30.0$	0.84	1.4	0.53	1.5	
p=20 ($\bar{\tau}=5.0\times10^{-9}$ sec)					
$D_1=1.2$, $D_2=5.0$, $D_3=10.0$, $D_4=30.0$	2.39	1.8	2.13	1.9	66
$D_1=1.2$, $D_2=10.0$, $D_3=10.0$, $D_4=30.0$	2.69	1.8	2.42	1.9	83
p=50 ($\bar{\tau}=5\times10^{-9}$ sec)					
$D_1=1.2$, $D_2=5.0$, $D_3=10.0$, $D_4=30.0$	5.32	2.0	5.12	1.9	
$D_1=1.2$, $D_2=10.0$, $D_3=10.0$, $D_4=30.0$	6.11	2.0	5.86	1.9	

[a] Log-χ^2 distribution assumed; all Di's are given in units of 10^{10} sec^{-1}.

[b] Listed diffusion coefficients reproduce observed data for the stated experimental temperatures.

TABLE 23. CALCULATED METHYLENE SPIN-LATTICE RELAXATION TIMES AND NUCLEAR OVERHAUSER ENHANCEMENT FACTORS FOR THE C-5 CARBON

	67.9 MHz		22.6 MHz	
Distribution Width[a]	T_1(sec)	NOEF(η)	T_1(sec)	NOEF(η)
p=8 ($\bar{\tau}=1.3\times10^{-7}$ sec)				
$D_1=D_2=D_3=D_4=D_5=1.0$	0.43	1.3	0.25	1.4
$D_1=D_2=D_3=1.0$, $D_4=4.0$, $D_5=7.0$	0.68	1.3	0.46	1.4
$D_1=D_2=D_3=D_4=D_5=10.0$	1.43	1.4	0.91	1.5
p=20 ($\bar{\tau}=5.0\times10^{-9}$ sec)				
$D_1=D_2=D_3=D_4=D_5=1.0$	0.74	1.7	0.60	1.8
$D_1=D_2=D_3=1.0$, $D_4=4.0$, $D_5=7.0$	1.50	1.8	1.29	1.9
$D_1=D_2=D_3=D_4=D_5=10.0$	5.25	1.9	4.88	1.9

[a] Log-χ^2 distribution assumed; all Di's are given in units of 10^{10} sec^{-1}.

CONCLUSIONS

^{13}C and ^{15}N Fourier transform nmr spectroscopies have shown their potential as powerful probes of toxic environmental chemicals. These two related spectroscopic techniques can perform chemical structure elucidation and, moreover, they can be used to probe physico-chemical interactions between environmental contaminants and model bio-systems (i.e., lipid bilayers). For some important environmental studies spectrometer sensitivity must be extended past the state-of-the-art; this is particularly true for ^{15}N work at natural (0.36%) isotopic abundance.

A number of general nmr techniques were developed for this project. They include improved methods for performing quantitative nmr analysis, relaxation experiments, and ^{15}N detection. A semi-quantitative analysis was demonstrated for polychlorinated biphenyl mixtures not requiring prior separation of individual species.

The joint use of 21.3 and 63.4kGauss magnetic fields to determine ^{13}C relaxation data allowed a new analysis of complex motions of alkyl chains in various molecular systems, including model membrane systems. This work should allow future detailed analysis of the disruption of membrane function when chemical contaminants are incorporated into bilayer structures.